

# Cdc6 expression represses E-cadherin transcription and activates adjacent replication origins

Maria Sideridou,<sup>1</sup> Roubini Zakopoulou,<sup>1</sup> Konstantinos Evangelou,<sup>1</sup> Michalis Lontos,<sup>1</sup> Athanassios Kotsinas,<sup>1</sup> Emmanouil Rampakakis,<sup>2,3</sup> Sarantis Gagos,<sup>4</sup> Kaoru Kahata,<sup>6</sup> Kristina Grabusic,<sup>8</sup> Kalliopi Gkouskou,<sup>9,10</sup> Ioannis P. Trougakos,<sup>11</sup> Evangelos Kolettas,<sup>12,13</sup> Alexandros G. Georgakilas,<sup>14</sup> Sinisa Volarevic,<sup>7</sup> Aristides G. Eliopoulos,<sup>9,10</sup> Maria Zannis-Hadjopoulos,<sup>2,3</sup> Aristidis Moustakas,<sup>6,7</sup> and Vassilis G. Gorgoulis<sup>1,5</sup>

<sup>1</sup>Molecular Carcinogenesis Group, Department of Histology and Embryology, School of Medicine, University of Athens, 11527 Athens, Greece

<sup>2</sup>Goodman Cancer Center and <sup>3</sup>Department of Biochemistry, McGill University, Montreal, Quebec H3G 1Y6, Canada

<sup>4</sup>Laboratory of Genetics, <sup>5</sup>Biomedical Research Foundation, Academy of Athens, 11527 Athens, Greece

<sup>6</sup>Ludwig Institute for Cancer Research, Biomedical Center; and <sup>7</sup>Department of Medical Biochemistry and Microbiology, Science for Life Laboratory; Uppsala University, SE-751 23 Uppsala, Sweden

<sup>8</sup>Department of Molecular Medicine and Biotechnology, School of Medicine, University of Rijeka, HR-51000 Rijeka, Croatia

<sup>9</sup>Molecular and Cellular Biology Laboratory, Division of Basic Sciences, University of Crete Medical School, 71003 Heraklion, Crete, Greece

<sup>10</sup>Institute for Molecular Biology and Biotechnology, Foundation of Research and Technology–Hellas, GR-70013 Heraklion, Crete, Greece

<sup>11</sup>Department of Cell Biology and Biophysics, Faculty of Biology, University of Athens, GR-15784 Athens, Greece

<sup>12</sup>Cell and Molecular Physiology Unit, Department of Physiology, School of Medicine, University of Ioannina, 451 10 Ioannina, Greece

<sup>13</sup>Biomedical Research Institute, Foundation of Research and Technology–Hellas (FORTH), GR-451 10 Ioannina, Greece

<sup>14</sup>Department of Biology, Thomas Harriot College of Arts and Sciences, East Carolina University, Greenville, NC 27858

**E**-cadherin (*CDH1*) loss occurs frequently in carcinogenesis, contributing to invasion and metastasis. We observed that mouse and human epithelial cell lines overexpressing the replication licensing factor Cdc6 underwent phenotypic changes with mesenchymal features and loss of E-cadherin. Analysis in various types of human cancer revealed a strong correlation between increased Cdc6 expression and reduced E-cadherin levels. Prompted by these findings, we discovered that Cdc6 repressed *CDH1* transcription by binding to the E-boxes of its promoter, leading to dissociation of the chromosomal

insulator CTCF, displacement of the histone variant H2A.Z, and promoter heterochromatinization. Mutational analysis identified the Walker B motif and C-terminal region of Cdc6 as essential for *CDH1* transcriptional suppression. Strikingly, CTCF displacement resulted in activation of adjacent origins of replication. These data demonstrate that Cdc6 acts as a molecular switch at the *E-cadherin* locus, linking transcriptional repression to activation of replication, and provide a telling example of how replication licensing factors could usurp alternative programs to fulfill distinct cellular functions.

## Introduction

DNA replication occurs once per cell cycle. Tight regulation of this process is controlled by the replication licensing machinery through periodic accumulation and destruction of the prereplicative complex (pre-RC), including among others, the Cdc6 (cell division cycle 6) protein (Lau et al., 2007; Borlado and Méndez, 2008). Cdc6 is a 60-kD protein that belongs to the AAA<sup>+</sup> (ATPases associated with various activities) family of ATPases

(Borlado and Méndez, 2008; Zachariadis and Gorgoulis, 2008). Deranged expression of pre-RC proteins, such as overexpression of Cdc6, leads to rereplication (Vaziri et al., 2003; Bartkova et al., 2006; Davidson et al., 2006; Lontos et al., 2007; Blow and Gillespie, 2008; Green et al., 2010), a form of replication stress, fuelling genomic instability, and promoting malignant behavior (Karakaidos et al., 2004; Lontos et al., 2007; Halazonetis et al., 2008; Negrini et al., 2010; Hanahan and Weinberg, 2011). In addition to this tumorigenic mechanism, Cdc6 has been reported to exert its oncogenic activity

M. Sideridou and R. Zakopoulou contributed equally to this paper.

Correspondence to Vassilis G. Gorgoulis: [vgorg@med.uoa.gr](mailto:vgorg@med.uoa.gr); or Aristidis Moustakas: [aris.moustakas@imbim.uu.se](mailto:aris.moustakas@imbim.uu.se)

Abbreviations used in this paper: ARF, alternative reading frame; CHIP, chromatin immunoprecipitation; EMSA, electrophoretic mobility shift assay; EMT, epithelial to mesenchymal transition; IF, immunofluorescence; LOH, loss of heterozygosity; M-FISH, multicolor FISH; pre-RC, prereplicative complex; RD, regulatory domain; SCID, severe combined immunodeficiency; TSA, trichostatin A.

© 2011 Sideridou et al. This article is distributed under the terms of an Attribution–Noncommercial–Share Alike–No Mirror Sites license for the first six months after the publication date [see <http://www.rupress.org/terms>]. After six months it is available under a Creative Commons License [Attribution–Noncommercial–Share Alike 3.0 Unported license, as described at <http://creativecommons.org/licenses/by-nc-sa/3.0/>].

Supplemental Material can be found at:  
<http://jcb.rupress.org/content/suppl/2011/12/22/jcb.201108121.DC1.html>

by repressing the *INK4/alternative reading frame (ARF)* locus (Gonzalez et al., 2006).

We have previously made the intriguing observation that Cdc6 overexpression in premalignant, nontumorigenic mouse epithelial cells leads to malignant transformation with features of epithelial to mesenchymal transition (EMT; Liontos et al., 2007). EMT is vital for tissue morphogenesis: it is pathologically activated in cancer and is marked by loss of the tumor suppressor E-cadherin (Hirohashi, 1998; Thiery et al., 2009). E-cadherin (*CDH1*) belongs to the superfamily of  $\text{Ca}^{2+}$ -dependent homophilic adhesion molecules. It is localized, together with the catenin complex, to the adherens junctions organizing interepithelial attachments (Hirohashi, 1998). Loss of E-cadherin expression follows the Knudson “two-hit” inactivation process of tumor suppressor genes in various (familial and nonfamilial) types of cancer and is associated with cancer invasion (Hirohashi, 1998). Biallelic inactivation involves combinations between mutations, deletions, aberrant endocytosis–proteolytic processing, and epigenetic silencing, with the last being a prominent event (Berox and van Roy, 2009 and references therein). Of note, in familial malignancies, such as diffuse gastric and lobular breast cancer, germline mutations are frequently complemented by *CDH1* promoter hypermethylation (Berox and van Roy, 2009 and references therein).

Our observations (Liontos et al., 2007) led us to hypothesize that tumorigenic Cdc6 may repress the *CDH1* locus. Here, we report a novel mechanism of E-cadherin suppression, mediated by Cdc6, which disrupts epithelial integrity and activates adjacent replication origins.

## Results

### Oncogenic Cdc6 represses E-cadherin

Extending our previous findings in P1 mouse cells (Liontos et al., 2007), we have found that stable expression of Cdc6 in A549 human lung carcinoma cells also results in loss of epithelial characteristics and acquirement of a mesenchymal phenotype (Fig. 1 a). Thus, Cdc6-transformed P1 and A549 cells displayed loss of membranous E-cadherin (Fig. 1, a and b), up-regulation of the mesenchymal markers, N-cadherin, vimentin, and fibronectin (Fig. 1 a), and a shift of membranous  $\beta$ -catenin to the cytoplasm and nucleus (Fig. 1 b). As a control (Gonzalez et al., 2006), *INK4* levels were also decreased in P1-Cdc6 cells (Fig. 1 b).

The Cdc6-transfected cells migrated and proliferated faster than their control (Mock) counterparts (Fig. 1, c and d), were more invasive, and formed larger and more colonies in soft agar (Fig. 1, e and f). Grafted A549-Cdc6 cells generated tumors in severe combined immunodeficiency (SCID) mice faster than control counterparts (Fig. 2 a). In addition, only the P1-Cdc6 cells formed tumors, as the P1 control cells are nontumorigenic (Fig. 2 b). Cdc6-driven tumors were almost completely E-cadherin negative and demonstrated predominantly mesenchymal features, such as spindle cell morphology and a partial (in A549-Cdc6) or complete (in P1-Cdc6) intermediate filament shift from cytokeratin to vimentin (Fig. 2). Importantly, the inverse connection between

Cdc6 and E-cadherin expression was also apparent in various human tumors, as depicted by serial section immunohistochemical analysis (Fig. 3, Table S1, and Table S2). The corresponding adjacent normal epithelia served as negative and positive internal controls for Cdc6 (Liontos et al., 2007) and E-cadherin, respectively (Fig. 3).

In support of the central role of Cdc6 in *CDH1* regulation, siRNA-mediated Cdc6 silencing reestablished the epithelial, E-cadherin–positive phenotype (Fig. 4, a and b). This was also shown in A549 cells expressing a tetracycline-inducible Cdc6. Upon Cdc6 induction, the cells attained a mesenchymal E-cadherin–negative phenotype, which was reversed (MET) when exogenous Cdc6 expression was switched off (Fig. 4 c). From the aforementioned findings, we conclude that E-cadherin suppression by Cdc6 (reversible change) is independent from Cdc6-driven genetic (irreversible) alterations. The ability of increased Cdc6 expression to trigger genomic instability was confirmed in the present study, in line with previous studies (see Introduction, Fig. S1, and Fig. S2). In comparison with the morphological changes that occurred within a short time period (Fig. 4), genomic instability was evident only after a longer period of cultivation (Fig. S1 and Fig. S2). A noteworthy observation of our molecular cytogenetic analysis was that the *p53* locus suffered allelic loss in both P1 and A549 Cdc6-transformed cells (Fig. S2 c).

Collectively, these data demonstrate a novel role for Cdc6 as a negative regulator of E-cadherin expression. Subsequently, the mechanism underlying E-cadherin down-regulation by Cdc6 was addressed.

### Cdc6 represses E-cadherin by binding directly to the E-boxes of the *CDH1* promoter

Transient expression of Cdc6 was followed by reduction of E-cadherin at the protein and mRNA level in all cell lines investigated (P1, MCF7A, MDCK, and immortalized human bronchial epithelial [HBEC3-KT] cells; Fig. 5), suggesting that regulation occurs at the transcriptional level. The latter was further examined with a luciferase reporter harboring 1.484 kb of 5'-flanking sequences, spanning the regulatory elements of *CDH1* (Fig. 6 a; Peinado et al., 2004; Berx and van Roy, 2009). The activity of the *CDH1* promoter-driven luciferase reporter showed a significant decrease when cotransfected with Cdc6 (Fig. 6 a). The extent of reduction was slightly higher than that obtained by a reporter driven by the *regulatory domain (RD)* of *INK4/ARF* used as a positive control (Fig. 6 a; Gonzalez et al., 2006). This *RD* element was identified during an experimental survey for regulatory elements proximal to replication origins of the *INK4A/ARF* locus. It turned out to be conserved in mammals and to coincide with a replication origin 1.5 kb upstream of this locus. Based on the aforementioned observations and because tethering of Cdc6 to DNA stimulates pre-RC assembly and replication initiation (Takeda et al., 2005), we searched for origins adjacent to the *CDH1* promoter that could also act as regulatory elements. To this end, we quantified nascent DNA products in a 10-kb region flanking it, in both P1 and A549 lines. Interestingly, abundant nascent DNA levels originating

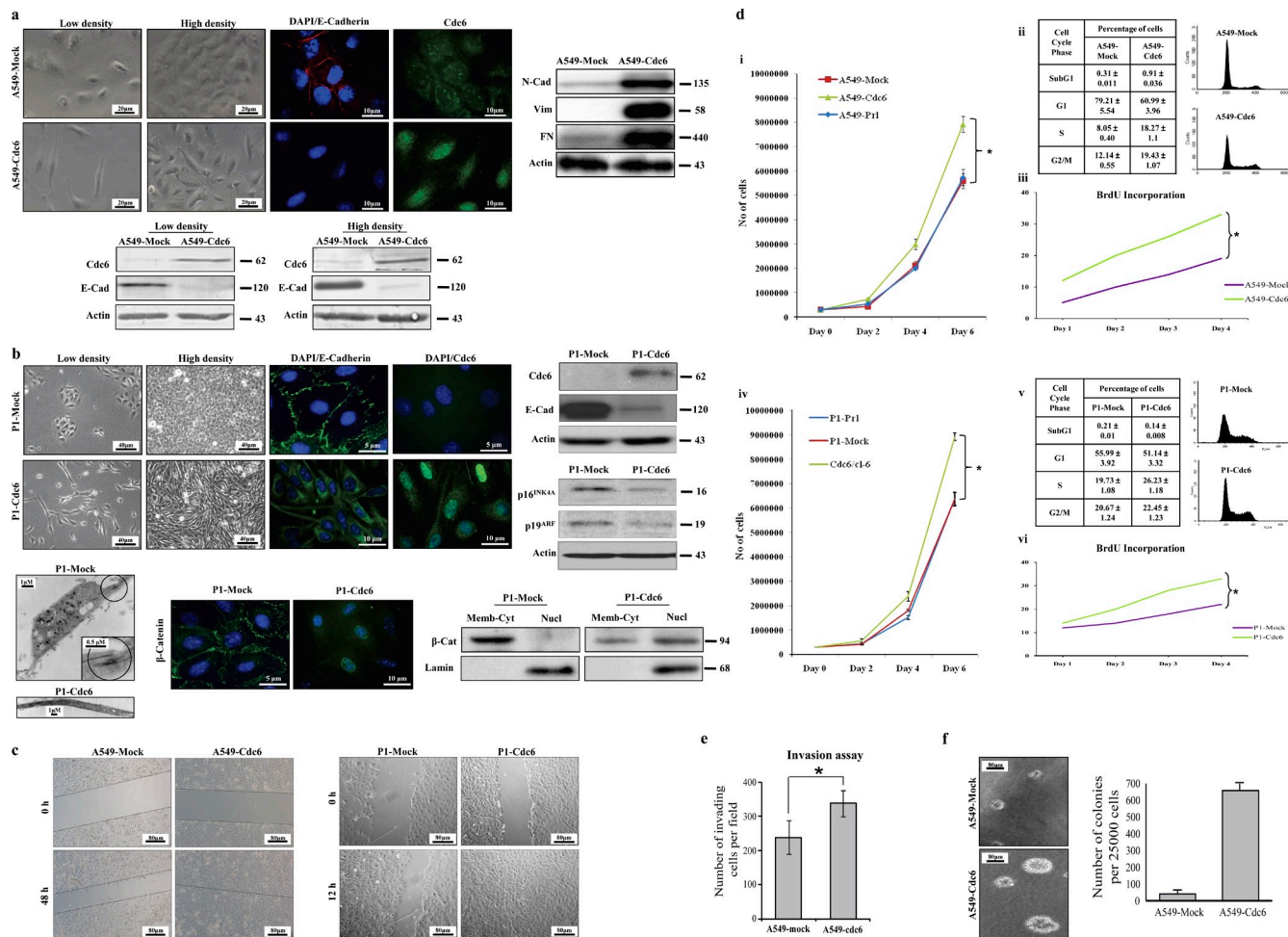


**Figure 1. Overexpression of Cdc6 represses E-cadherin.** (a) Loss of membranous localization, decreased expression of E-cadherin (E-cad), and spindle morphology in A549-Cdc6 cells. The mesenchymal markers N-cadherin (N-cad), vimentin (vim), and fibronectin (FN) are up-regulated and accompany Cdc6 overexpression. (b) Similar morphological features and E-cadherin loss appear in P1-Cdc6 cells along with decreased  $p16^{INK4A}$  and  $p19^{ARF}$  levels. Ultrastructural features, such as loss of desmosomes (circled inset photo) and elongated shape, further confirm morphological changes. Shift of membranous (Memb)  $\beta$ -catenin ( $\beta$ -cat) to the cytoplasm (Cyt) and nucleus (Nucl) of Cdc6 cells. Because the *INK4* locus is deleted in A549 cells (Pineau et al., 2003), the impact of Cdc6 overexpression on INK4 products could not be determined. (c) A549- and P1-hCdc6 cells migrate faster than corresponding control (Mock) cells for the indicated time points after an induced scratch. (d) Cdc6 overexpression confers a growth advantage to P1 and A549 cells. (i and iv) Growth curves of A549- and P1-Cdc6 Mock and parental (Pr1) cells (\*,  $P \leq 0.01$ ). (ii–vi) Tables depict FACS results (ii and v), whereas line plots show BrdU incorporation of the same P1- and A549-Cdc6 cells (iii and vi) in comparison with their corresponding control (Mock) cells (\*,  $P \leq 0.01$ ). (e) A549-Cdc6 cells are more invasive in the matrigel assay than the corresponding A549-Mock cells. Mean values from triplicate fields are plotted with SDs (\*,  $P < 0.05$ ). (f) A549-Cdc6 clones form more and larger colonies than the A549-Mock cells in soft agar assay ( $P < 0.001$ ). Molecular markers are given in kilodaltons.

from a single region immediately next to the *CDH1* promoter were uncovered (position  $-495$  in P1 cells and  $-286$  in A549; Fig. 6, b and c; Fig. S3; and Table S4). Of note, P1-Cdc6 cells exhibited activation of a dormant origin of replication because almost no nascent DNA originated from this site in Mock cells (Fig. 6 b and Fig. S3). However, an enhancement of the already active replication origin was found in A549-Cdc6 transfectants (Fig. 6 c and Fig. S3).

In contrast to the *RD* element, which is conserved among mammals, the human and mouse *CDH1* replication origins do not show any sequence similarities. Yet, sequence alignment of the *RD* element and the *CDH1* promoter identified conservation of the consensus CANNTG motif (Fig. 6 d). Intriguingly, this element matches the E-box sequence, the major cis-acting negative regulatory element of *CDH1* (Hajra et al., 1999; Li et al., 2000). We therefore reasoned that

Cdc6 could directly suppress *CDH1* by binding to the *CDH1* promoter E-boxes. Indeed, Cdc6 expression decreased *CDH1* promoter-driven luciferase reporter activity in various cell lines, whereas a promoter construct carrying mutated E-boxes remained unresponsive (Fig. 6 e). To further validate this finding we generated recombinant full-length Cdc6 protein (Fig. S4, a–c) and tested its capacity to bind to the E-box sequence. Using electrophoretic mobility shift assays (EMSA), we found that recombinant Cdc6 binds specifically to the wild-type E-box element but not to a mutated E-box (Fig. 6 f). Moreover, a specific band shift was noticed when protein extracts from the Cdc6-transformed cells, but not from the control (Mock) ones, were incorporated in a reaction containing the E-box 1 and E-pal elements (palindromic sequence composed of two adjacent E-boxes of the mouse *CDH1* promoter; Peinado et al., 2004) of the human and mouse E-cadherin promoters,

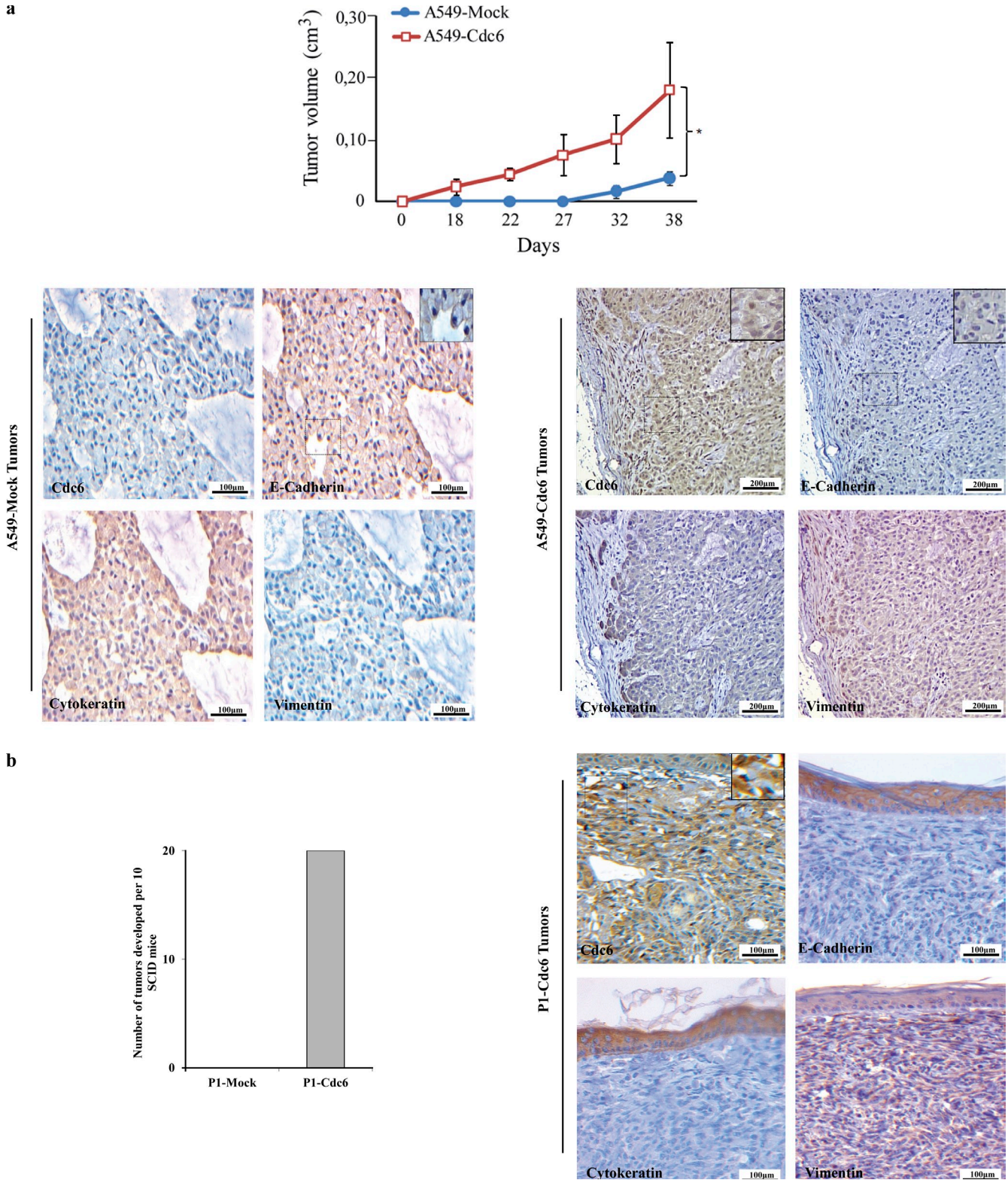


Figure 2. **Tumor formation of grafted A549- and P1-Cdc6 cells in SCID mice.** (a) Subcutaneously injected A549-Cdc6 cells form faster tumors than the Mock cells. Graph shows a single round of five animals (7-wk-old male SCID mice) per each cell type, which were subcutaneously injected on the left dorsal flank. Presence of E-cadherin and cytokeratin staining in A549-Mock-derived tumors. Absence of E-cadherin and partial intermediate filament shift from cytokeratin to vimentin in tumors generated from A549-Cdc6-grafted cells in SCID mice. The asterisk denotes a statistically significant result. (b) Only the P1-Cdc6 cells formed tumors because the P1-Mock cells are nontumorigenic. Graph shows a single round of five animals (7-wk-old male SCID mice) per each cell type, which were subcutaneously injected at two sites in the abdominal region. Absence of E-cadherin and complete intermediate filament shift from cytokeratin to vimentin in tumors generated from P1-Cdc6-grafted cells in SCID mice. Insets depict magnifications of the dotted rectangular areas. Error bars indicate SDs (\*,  $P < 0.01$ ).

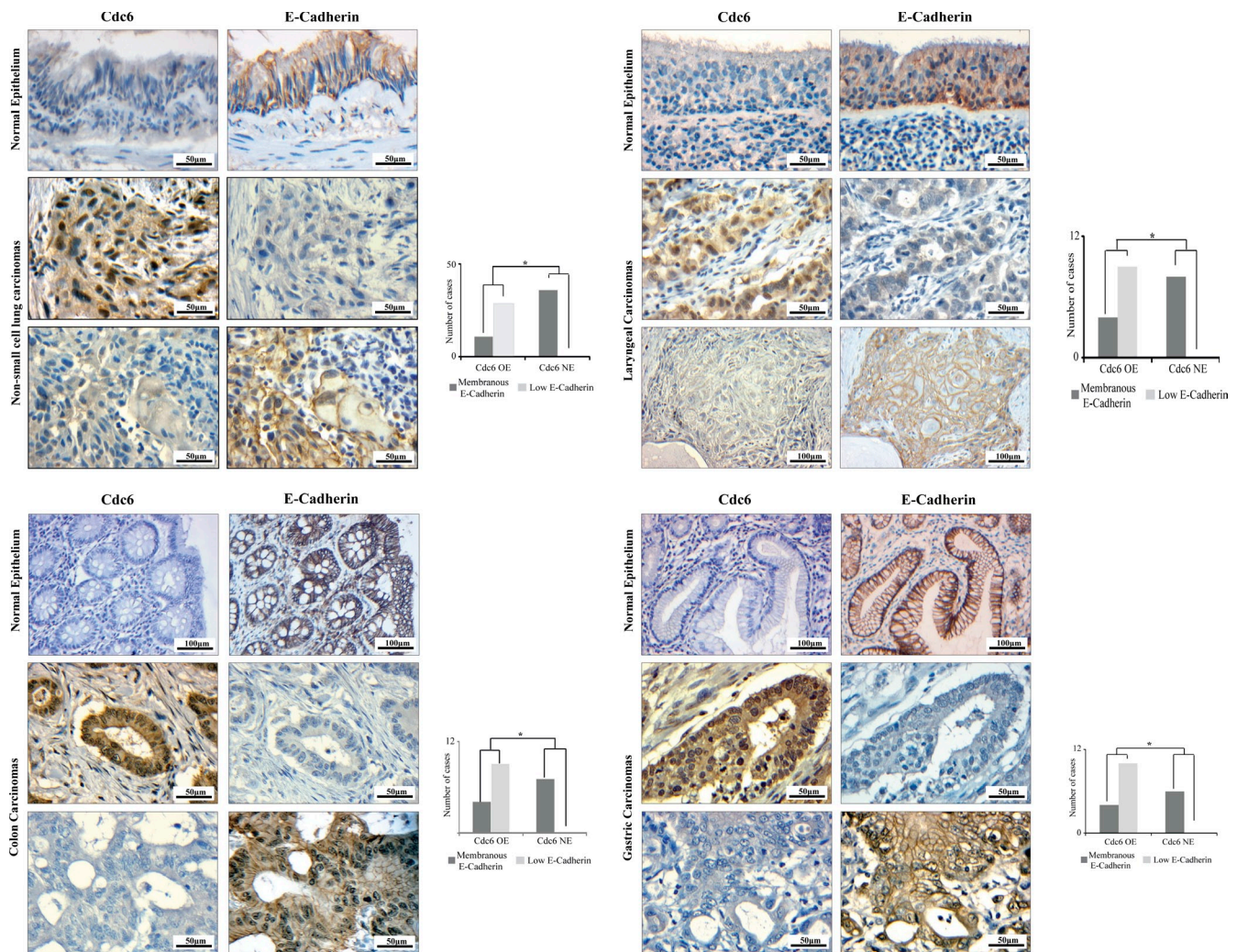


Figure 3. **Inverse relationship between E-cadherin and Cdc6 expression in human tumors.** Immunohistochemical analysis on serial sections from human lung, laryngeal, colon, and gastric carcinomas. Graphs plot the number of individual human tumors that exhibit membranous E-cadherin versus cytoplasmic/reduced E-cadherin and their relation to the levels (OE, overexpressed; NE, normal expression) of Cdc6 (\*,  $P < 0.001$ ). Corresponding normal epithelia that serve as internal positive controls for E-cadherin and negative controls for Cdc6 in relation to their corresponding adjacent carcinomas are also shown.

respectively (Fig. S4, d and e; and Table S5). Competition with molar excess of unlabeled, but mutated, E1-box and E-pal elements did not affect binding, whereas the band was supershifted when an N-terminal anti-Cdc6 antibody was included in the reaction mixture, confirming the presence of Cdc6 in the DNA-protein complex (Fig. S4, d and e). We conclude that the binding of Cdc6 to E-boxes associates with its capacity to suppress *CDH1* transcriptional activation.

#### Binding of Cdc6 to the E-boxes displaces the chromosomal insulator CTCF and histone H2A.Z triggering *CDH1* promoter heterochromatinization

In line with the EMSA data, chromatin immunoprecipitation (ChIP) assays in Cdc6-transformed cells demonstrated binding of myc-tagged Cdc6 to the chromatin regions containing the E-pal element and the E-boxes 1 and 3 from the mouse and human *CDH1* promoter, respectively (Fig. 7 a, middle box; and Table S3). The *RD<sup>INK4A/ARF</sup>* element was used as a positive

control, whereas distal regions served as negative controls (Fig. 7 a, left box and top right box, respectively). It has recently been reported that the epigenetic silencing of the tumor suppressor genes *p16<sup>INK4A</sup>*, *RASSF1A*, and *CDH1* depends on the binding of the CTCF insulator to chromosomal boundaries, acting as a barrier against the spread of heterochromatin (Witcher and Emerson, 2009). In silico analysis using the CTCFBSDB tool (Bao et al., 2008) indicated the presence of CTCF binding sites in the human and mouse *CDH1* promoters. Sequence alignment of the mouse and human *CDH1* promoter regions showed that in both species the CTCF regulatory sites colocalize with the E-pal and the E-box 1, respectively (Fig. 7 b). Moreover, a recent study reported that CTCF binding sites are flanked by nucleosomes enriched for the histone variant H2A.Z, which possesses an antisilencing role (Fu et al., 2008). Prompted by these observations, we tested whether Cdc6 removes CTCF and H2A.Z from the *CDH1* promoter, promoting heterochromatinization of the region. Indeed, ChIP analysis revealed that CTCF and H2A.Z were displaced

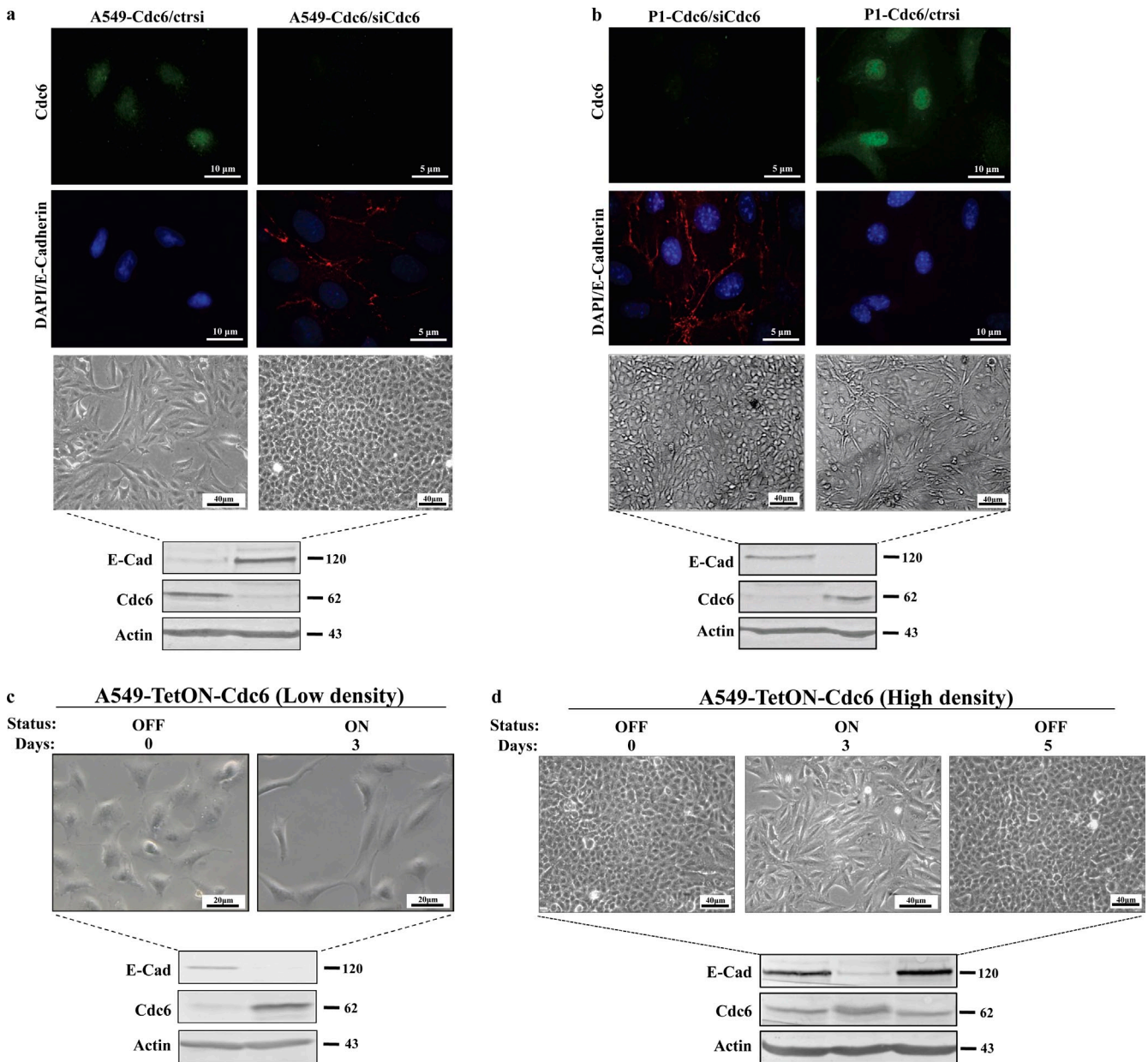


Figure 4. **Cdc6-mediated E-cadherin suppression is reversible.** (a) Cdc6 siRNA in A549-Cdc6 cells restored the epithelial E-cadherin (E-Cad)-positive phenotype. (b) Similar effect in P1-Cdc6 cells. (c and d) Induction of Cdc6 expression in the A549-TetON-inducible cells (for 3 d) led to E-cadherin down-regulation and to a spindle phenotype that are reversed after shutting down Cdc6 (for an additional 5 d). A549-TetON Cdc6 low density cells were continuously passaged to avoid aggregation. ctrsi, control siRNA. Molecular markers are given in kilodaltons.

from the *CDH1* promoter in Cdc6-transformed cells (Fig. 7 a, middle box). These chromatin modifications were accompanied by hypoacetylation of histones H3 and H4 (Fig. 7 a, middle box), suggesting a histone deacetylase recruitment in the region enclosing the E-boxes. Treatment with the histone deacetylase inhibitor trichostatin A (TSA) prevented Cdc6-induced deacetylation of the *CDH1* promoter, supporting this notion (Fig. 7 a, bottom right box). Subsequently, signs of heterochromatinization, as depicted by increased H3K9me3, were identified (Fig. 7 a, middle box). Similar results were obtained after transient expression of myc-tagged Cdc6 in MCF7A cells (Fig. 7 a, middle box).

Overall, these data clearly support a model in which binding of Cdc6 is followed by regional chromatin reorganization

shutting down E-cadherin expression. Further support for this novel mechanistic model emerges from the fact that siRNA silencing of CTCF represses E-cadherin transcription (Fig. 7 c).

#### The Walker B motif and C-terminal region of Cdc6 are essential for CDH1 suppression

Sequencing of Cdc6 in tumors has so far failed to identify mutations, implying that its structural integrity is vital for its function (Blow and Gillespie, 2008). Cdc6 includes several conserved and functionally important motifs (Borlado and Méndez, 2008; Zachariadis and Gorgoulis, 2008). The N terminus

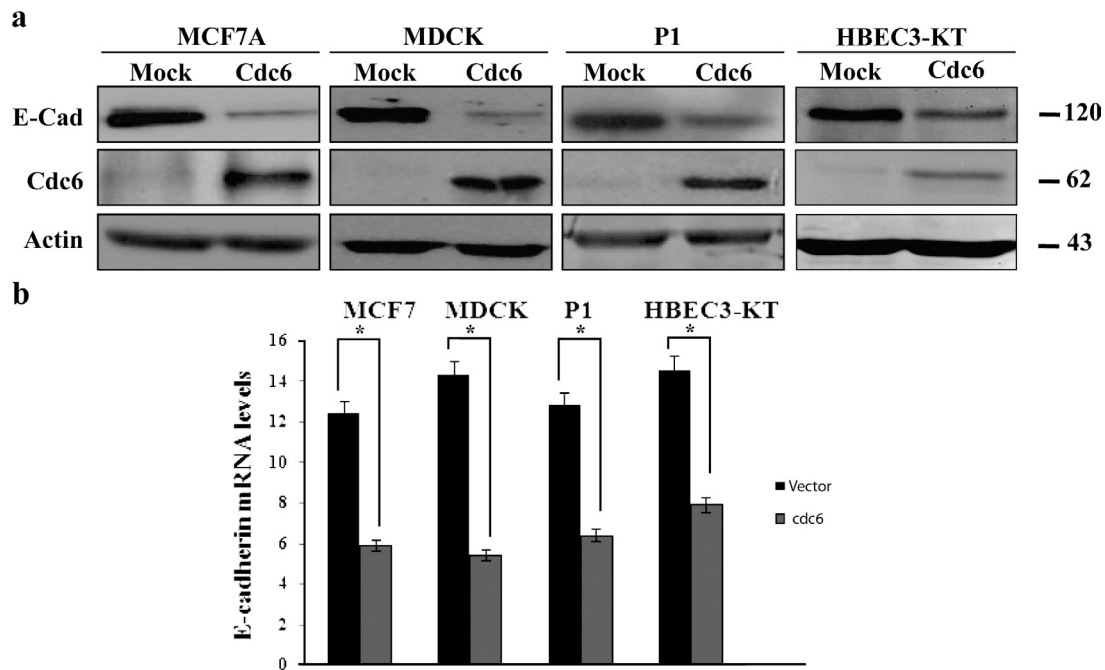


Figure 5. **Cdc6 transcriptionally represses E-cadherin.** (a and b) E-cadherin (E-Cad) protein (a) and mRNA (b) level reduction in MCF7A, MDCK, P1, and HBEC3-KT cells after transient Cdc6 expression. The asterisk denotes a statistically significant result. Error bars indicate SDs. Molecular markers are given in kilodaltons.

contains three consensus phosphorylation sites at S54, S74, and S106, which are nodal for Cdc6 protein turnover (Fig. 8 a). Mutating S54, S74, and S106 to alanines (Cdc6-AAA) or truncating the N terminus ( $\Delta 125$ -Cdc6/ $\Delta$ NH<sub>2</sub>-Cdc6; Fig. 8 a) partly compromised the suppressive effect on *CDH1* (Fig. 8 b), whereas these mutations had no effect on *INK4* repression (Gonzalez et al., 2006). Of note, removal of the N-terminal 125-amino acid region ( $\Delta 125$ ) produced a nondegradable form of Cdc6, which however, was unable to suppress *CDH1* to the extent that wild-type Cdc6 did (Fig. 8 b). Therefore, the N-terminal region possesses features that influence the chromatin-remodeling capacity of Cdc6.

The central portion of Cdc6 harbors the Walker A (amino acids 202–209) and Walker B (amino acids 284–287) motifs, which bind and hydrolyze ATP, respectively. Substituting D284A and D285A in the Walker B motif (Cdc6-W<sup>B</sup>) almost abolished the suppressive effect on *CDH1* expression (Fig. 8 b).

The C-terminal Cdc6 domain encompasses among others a conserved winged helix domain that is present in several DNA-binding proteins (Borlado and Méndez, 2008). Deleting the C-terminal domain ( $\Delta 440$ –560) of Cdc6 (Cdc6- $\Delta$ COOH; Fig. 8 a) abolished the suppressive effect on *CDH1* (Fig. 8 c). Interestingly, expression of this construct was accompanied by increased apoptosis (Fig. 8 d), which is in agreement with the described ability of the caspase-cleaved isoform lacking the same domain to promote cell death (Pelizon et al., 2002). The expression levels of the Cdc6- $\Delta$ COOH mutant were considerably lower than those of the  $\Delta 125$ -Cdc6 mutant (Fig. 8 c), highlighting the importance of the C-terminal domain for both repressive ability and stability.

The corresponding luciferase and ChIP assays with the Cdc6 mutants paralleled that of E-cadherin expression analysis

(Fig. 8, e and f). Collectively, the functional analysis of the Cdc6 mutants revealed that the Walker B motif and C-terminal portion of Cdc6 are indispensable for *CDH1* suppression.

#### Displacement of CTCF by Cdc6 links transcriptional repression of *CDH1* with activation of adjacent replication origins

Cancer adopts embryonic programs, such as EMT, necessary for its progression. Moreover, changes in origin selection, localization, and temporal activation occur during embryonic development and are often linked to gene expression (Norio et al., 2005; Grégoire et al., 2006). Given that *CDH1* suppression is essential for EMT, colocalization of genes, such as *CDH1* and *INK4/ARF*, with origins of replication implies a mutually exclusive functional relationship between replication firing and activation of genes related with growth inhibition and/or differentiation. We therefore asked whether Cdc6-mediated E-cadherin suppression and Cdc6-triggered activation of the adjacent replication origins are intertwined or whether they are coincidental.

Using the tetracycline-regulated Cdc6 in A549 cells, we observed down-regulation of E-cadherin upon induction of Cdc6, which was accompanied by a threefold enhancement of replication origin activity. Conversely, shutting down Cdc6 was followed by reestablishment of E-cadherin and decreased activity of the replication origin (Fig. 9 a). Notably, Cdc6 overexpression only marginally increased the activities of the replication origins of the *Lamin B2* and *HPRT* genes, which were used as positive controls (Fig. 6, b and c; Falaschi et al., 2007), suggesting that oncogenic Cdc6 does not activate all origins uniformly but targets specific replication sites.

The binding activity of CTCF to the *CDH1* promoter followed the fluctuations of the E-cadherin levels (Fig. 9 b).

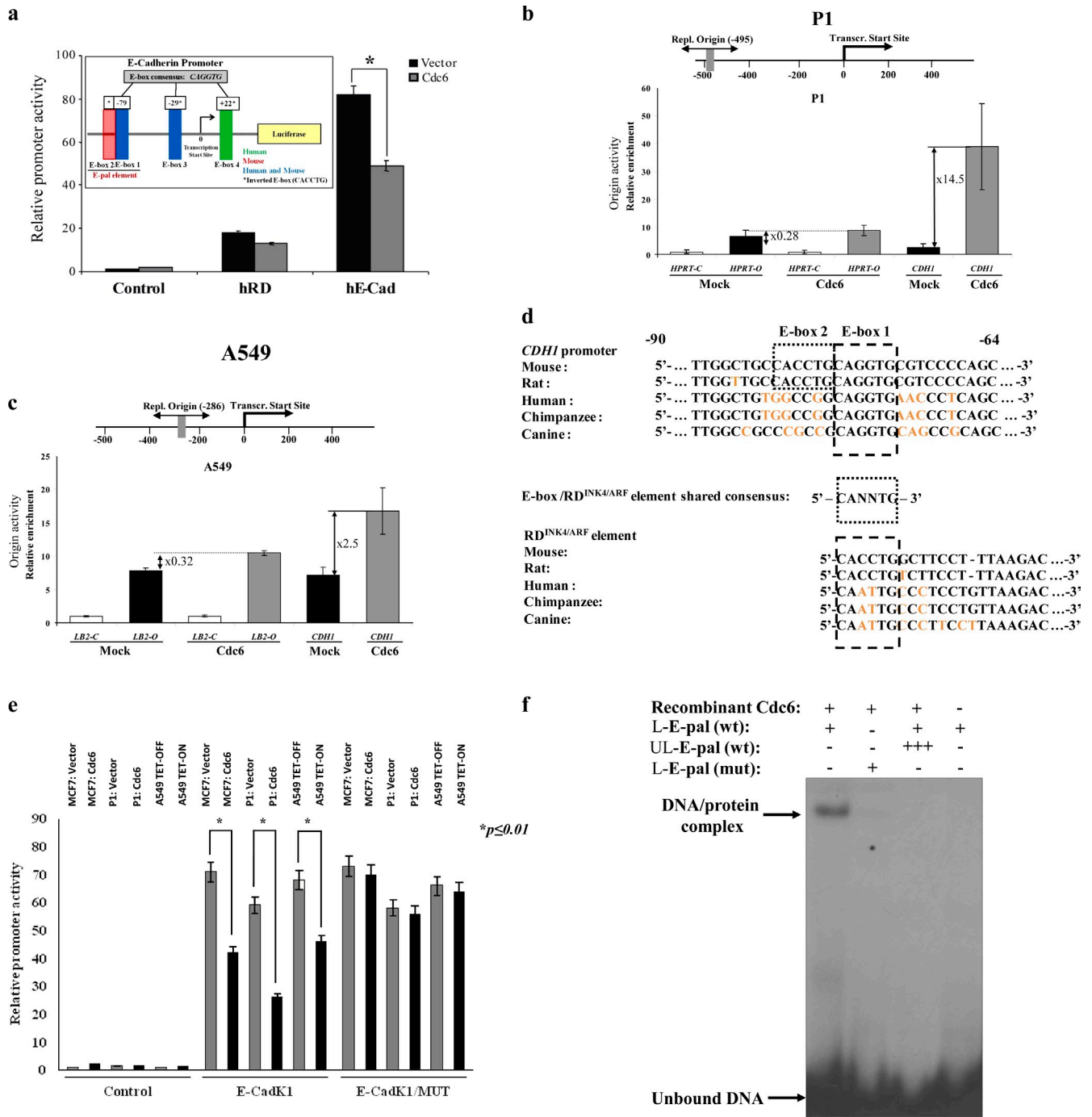


**Figure 6. Cdc6 represses E-cadherin by binding the E-boxes of the CDH1 promoter.** (a) Decreased activity of the CDH1 promoter-driven luciferase reporter when cotransfected with Cdc6 in MCF7A cells (Table S6). The positive control was the regulatory domain (RD) of INK4/ARF. (inset) CDH1 promoter diagram with the E-boxes positioned (Peinado et al., 2004) and numbered as per the human CDH1 sequence (Bex and van Roy, 2009). The asterisk denotes a statistically significant result. hRD, human RD; hE-Cad, human E-cadherin. (b and c) Production of nascent DNA from a replication (Repl.) origin adjacent to the promoter of the mouse CDH1 gene, in P1-Cdc6 cells, in comparison with the corresponding Mock ones. The well-established replication origin of the HPRT gene was used as an internal control. Transcr., transcription. (c) Histograms depicting increased activation of an already active replication origin identified next to the promoter of the human CDH1 gene, in A549-Cdc6 cells, in comparison with the corresponding Mock ones. The well-established replication origin of the Lamin B2 gene was used as an internal control (C, control region, distal origin-lacking region; O, well-characterized replication origin in the HPRT and Lamin B2 genes). Values are expressed as relative enrichment of the origin-containing region compared with the origin-lacking regions and represent five experiments  $\pm$  1 SD. Numbers next to the bars in the histograms denote fold increase. Numbers on the axis above the histograms denote distance in base pairs. (d) Sequence homology based on a shared consensus between the E-cadherin E-box promoter and the RD<sup>INK4/ARF</sup> element in mammals (numbering as per the human CDH1 sequence; Bex and van Roy, 2009). Divergent nucleotides are colored. Note the rodent-specific presence of the E-pal element (E-box 2 [inverted E-box sequence]/E-box 1 sequence). (e) Luciferase assay of human CDH1 promoter construct with wild-type or mutated E-boxes (1, 3, and 4; Table S6) cotransfected with Cdc6 in MCF7A, P1, and induced A549-Tet-ON cells. (f) Radioactive EMSA with a full-length human recombinant Cdc6 protein (Table S5). The triple plus sign denotes addition in excess of oligonucleotide. L, labeled oligonucleotide; UL, unlabeled oligonucleotide; wt, wild type; mut, mutant. Error bars indicate SDs.

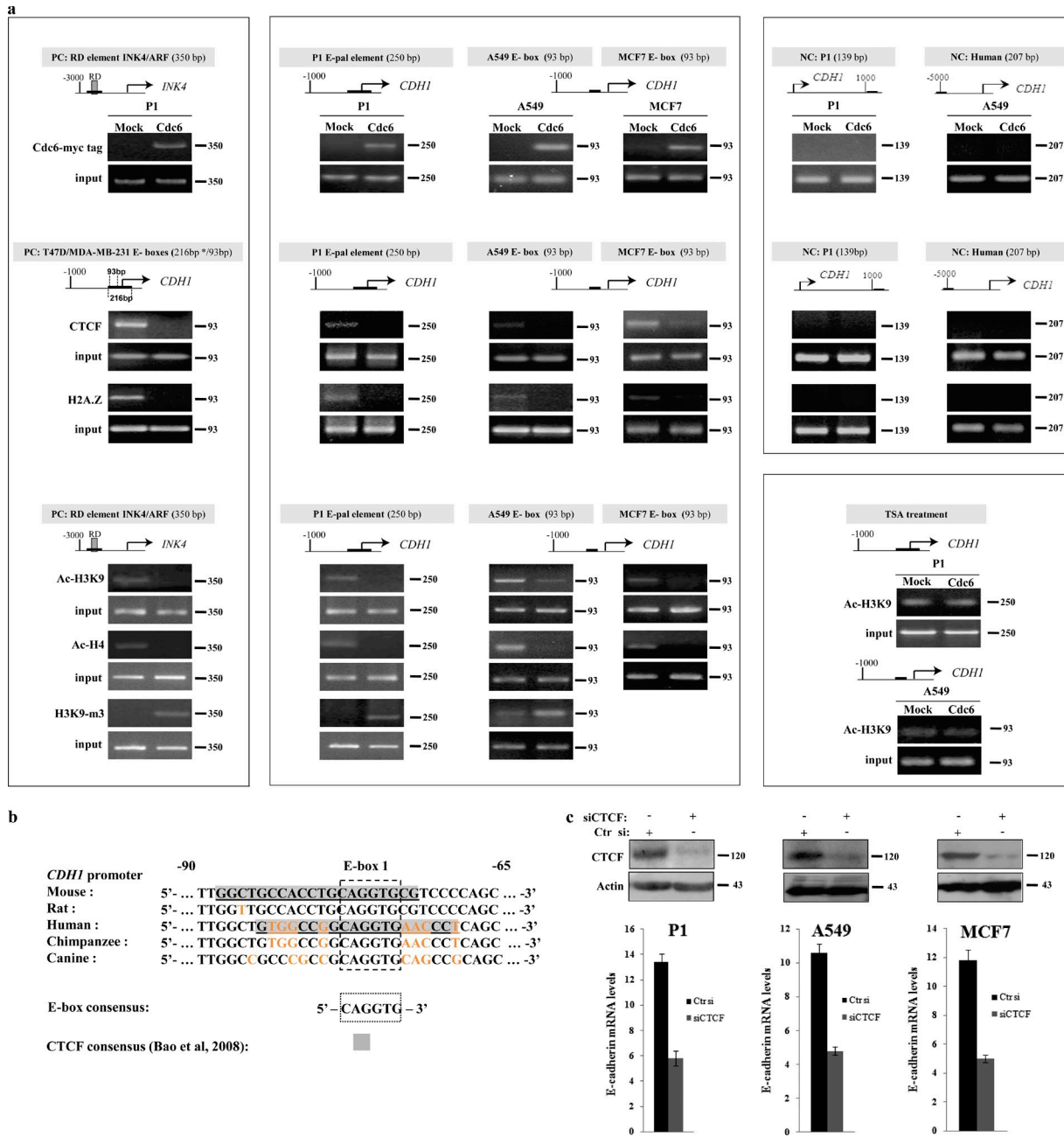
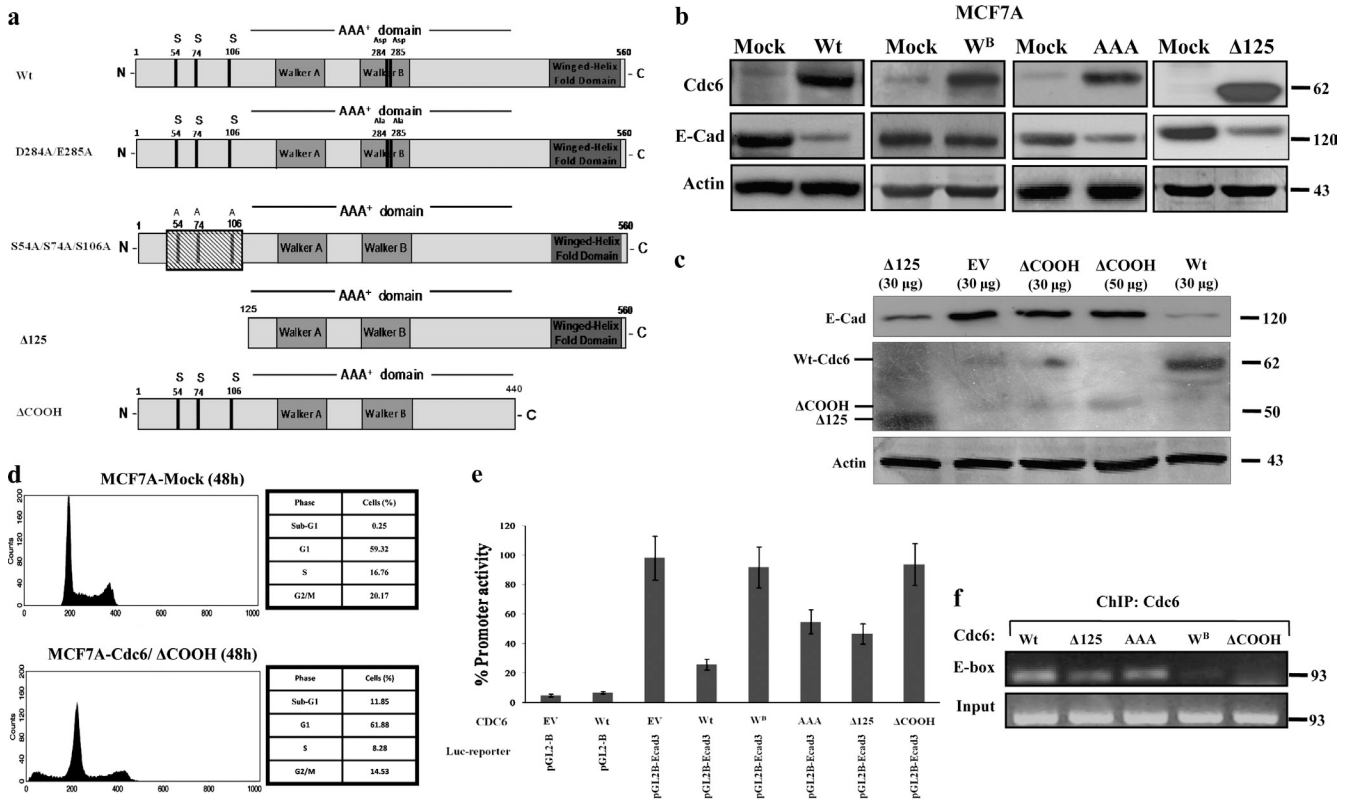


Figure 7. **Cdc6 triggers CDH1 promoter heterochromatinization by displacing the chromosomal insulator CTCF and the variant histone H2A.Z.** (a) ChIP for myc-tagged Cdc6 binding to the mouse E-pal element and human E-box 1 and 3. CTCF and H2A.Z histone displacement, hypoacetylation of histones H3 and H4, and increase in H3K9me3 in mouse and human cells (middle box). T47D and MDA-MB-231 were used as control cell lines (Witcher and Emerson, 2009; similar results were obtained with the primers encompassing the 216-bp region described by Witcher and Emerson [2009]; Table S3 and not depicted). The *RD<sup>INK4/ARF</sup>* element (PC, positive control; left box) and regions located 1.05 kb downstream of the E-pal element and 5 kbp upstream of the E-box (NC, negative control; top right box) were used as positive and negative controls, respectively. (bottom right box) TSA prevents Cdc6-induced deacetylation of the *CDH1* promoter. (b) Sequence homology between mammalian E-cadherin promoter regions encompassing E-box 1. CTCF-binding element is highlighted in gray. Divergent nucleotides are colored. (c) CTCF silencing leads to E-cadherin transcriptional repression. Ctr si, control siRNA. Error bars indicate SDs. Molecular markers are given in kilobases (a) and kilodaltons (c).

We thus surmised that displacement of CTCF by Cdc6 binding to the E-cadherin promoter results in *CDH1* silencing (Fig. 7, a and c), triggering activation of adjacent replication origins. Interestingly, we observed that silencing of CTCF, mimicking CTCF displacement, resulted in increased activity of the adjacent to the *CDH1* promoter origins of replication (Fig. 9 c). In line with this finding, CTCF has been reported to regulate the

asynchronous replication of the *H19/Igf2* locus, which is monoallelically expressed by delaying the replication of the CTCF-bound maternal allele (Bergström et al., 2007), and to reduce replication fork progression at the *DM1 (myotonic dystrophy type-1)* locus (Cleary et al., 2010).

We have also identified a putative CTCF binding site within the *RD<sup>INK4/ARF</sup>* element (Gonzalez et al., 2006; Bao et al., 2008)



**Figure 8. The Walker B motif and the C-terminal domain are essential for CDH1 suppression.** (a) Schematic presentation of Cdc6 mutants. Lined box denotes mutation of serines at codons 54, 74, and 106. N, N terminus; C, C terminus. (b) Effects of the Cdc6-W<sup>B</sup>, Cdc6-AAA, and Cdc6-Δ125 mutants on E-cadherin (E-Cad) protein level in MCF7A cells. (c) Inability of Cdc6-ΔCOOH to down-regulate E-cadherin. Cdc6-ΔCOOH mutant protein levels are considerably lower than the Cdc6-Δ125, indicating that the presence of the C-terminal domain is crucial for its stability. EV, empty vector. (d) Flow cytometric analysis of Cdc6-ΔCOOH-transfected MCF7A cells depicting increased apoptosis (increased sub-G1 phase). (e) Luciferase (Luc) activity of the CDH1 promoter-driven luciferase reporter when cotransfected with wild-type (Wt) and Cdc6 mutants in MCF7A cells. The binding capacity of the mutants followed their repressive activity (e). Error bars indicate SDs. Molecular markers are given in kilodaltons (b and c) and kilobases (f).

and found that silencing of CTCF enhances the activity of the replication origin previously identified within this element (Fig. 9 d; Gonzalez et al., 2006; Witcher and Emerson, 2009). Collectively, the aforementioned data suggest that the binding of oncogenic Cdc6 to the CDH1 locus leads to transcriptional repression of E-cadherin and the activation of adjacent origins of replication through displacement of CTCF.

## Discussion

Unraveling the mechanisms that neutralize tumor suppressor genes is fundamental in understanding carcinogenesis. E-cadherin is a key adhesion molecule frequently lost, by various means, in a range of epithelial malignancies and is considered as a tumor suppressor (Hirohashi, 1998; Berx and van Roy, 2009). The observation that cells overexpressing Cdc6 undergo EMT was unexpected and led us to the discovery of a novel mechanism of E-cadherin transcriptional repression mediated by Cdc6. The prominent reciprocal relationship between high Cdc6 levels and reduced E-cadherin expression, in different primary human tumors (Fig. 3), validates the clinical significance of this potential novel cancer-promoting mechanism.

Down-regulation of E-cadherin is considered a key initiating event in EMT, but sole suppression of E-cadherin does not

always suffice for EMT (Thiery et al., 2009). Indeed, we have observed that MCF7A cells stably expressing Cdc6 do not demonstrate features of EMT despite reduced E-cadherin levels (unpublished data). Interestingly, both P1 and A549 cells harbor mutated activated Ras (Liontos et al., 2007), a signaling pathway implicated in EMT (Turley et al., 2008), and it is thus likely that cooperation between Ras and Cdc6 composes a triggering event leading to EMT. In support of this hypothesis, Cdc6 overexpression cooperates with oncogenic Ras to transform mouse embryo fibroblasts (Gonzalez et al., 2006).

Various transcriptional repressors of E-cadherin have been previously described (Peinado et al., 2007). Our data suggest that oncogenic Cdc6 acts in a manner similar to the E-cadherin repressors Snail1/2, ZEB1/2, and E47, which bind directly to the E-boxes of the CDH1 promoter (Peinado et al., 2007). A nodal difference between Cdc6 and Snail is that Cdc6 confers a growth advantage in the cells that overexpress it, whereas Snail prevents entry into S phase by repressing cyclin D transcription (Vega et al., 2004). This discrepancy probably reflects their diverse physiological roles. Snail1 plays a vital part in gastrulation and neural crest development (Thiery et al., 2009), and by blocking S phase, it possibly synchronizes embryonic cell populations orchestrating the morphogenetic process. The periodical expression of Cdc6 secures physiological proliferation

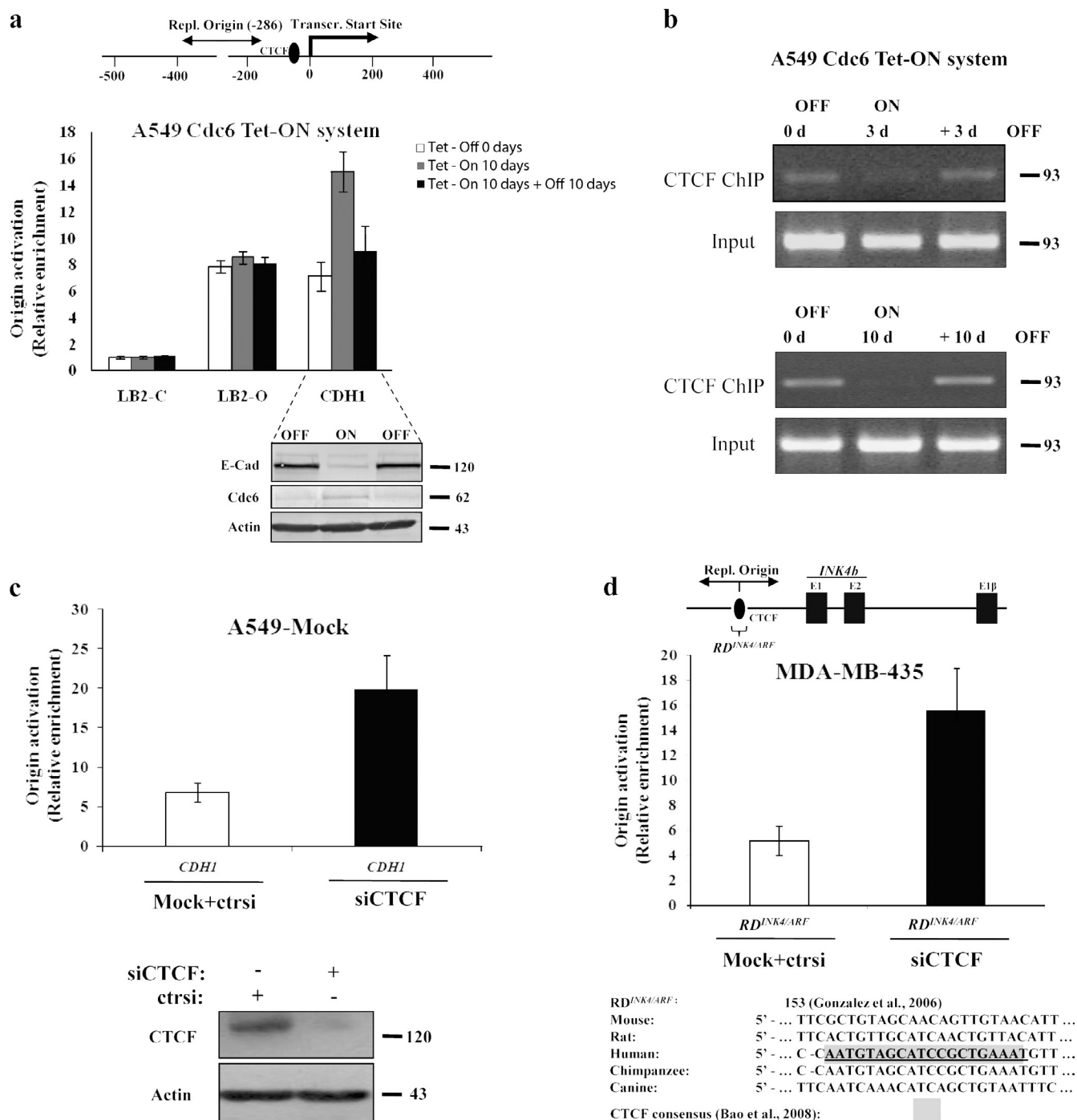


**Figure 9. CTCF displacement links Cdc6 overexpression with suppression of CDH1 and increased replication origin activity.** (a) E-cadherin (E-Cad) levels follow the activity of the replication (Repl.) origin located in the human *CDH1* promoter in induced and noninduced A549-Cdc6-Tet-ON cells (C, distal origin-lacking region; O, characterized *Lamin B2* gene replication origin; Transcr., transcription; Falaschi et al., 2007). (b) CTCF displacement from the *CDH1* promoter follows Cdc6 induction in A549-Cdc6-Tet-ON cells. CTCF ChIP assay in A549-Cdc6-Tet-ON cells induced and shut down at different time points. (c) Silencing of CTCF in A549-Mock cells activates the identified at the *CDH1* locus replication origin. (d) CTCF silencing in INK4A/ARF-expressing MDA-MB-435 cells activates the reported adjacent replication origin (Gonzalez et al., 2006). ctrlsi, control siRNA. Error bars indicate SDs. Molecular markers are given in kilodaltons (a and c) and kilobases (b).

by disallowing the detrimental process of rereplication (Lau et al., 2007); however, when Cdc6 is constantly overexpressed, this periodicity is lost, rendering the DNA prone to rereplication (Blow and Gillespie, 2008; Borlado and Méndez, 2008). This form of oncogene-induced replication stress will initially trigger the DNA damage response checkpoint, in an attempt to

repair generated DNA lesions, but eventually, selective pressure may disable its components, fuelling genomic instability and tumor growth (Halazonetis et al., 2008; Negrini et al., 2010). In line with this scenario, we observed allelic loss of *p53* in both P1 and A549 cells stably expressing Cdc6. The acquired growth advantage could be further stimulated by the

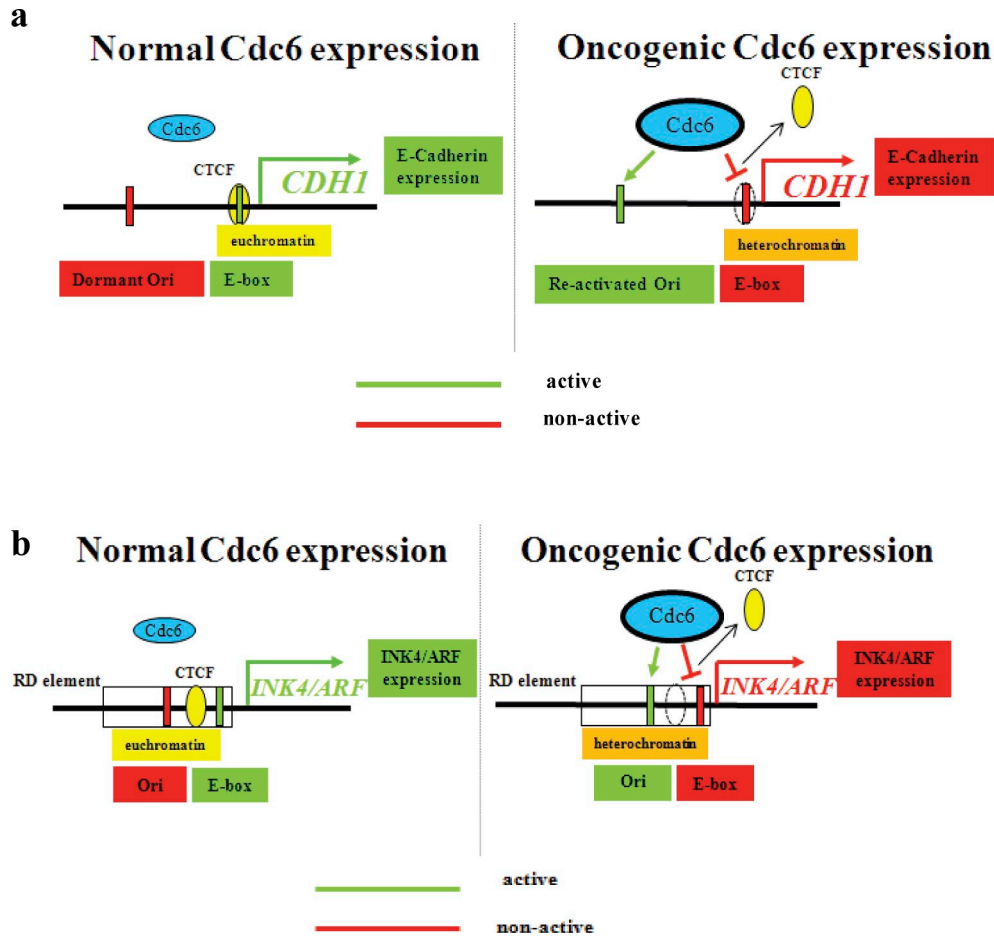


Figure 10. **Model describing the ability of oncogenic Cdc6 to act as a molecular switch.** (a and b) Cdc6 acting as a molecular switch at the *CDH1* (a) and *INK4/ARF* (b) locus (see Discussion). Ori, replication origin.

ability of Cdc6 to transcriptionally suppress the tumor suppressor genes, *p16<sup>INK4A</sup>*, *ARF* (Gonzalez et al., 2006), and *CDH1* (this paper). These oncogenic manifestations of Cdc6 function may have additional repercussions. If for example, in the appropriate cellular context and microenvironment, Cdc6-driven EMT/MET is used for invasion and metastasis, the metastatic (secondary) site may well resemble phenotypically the primary site, but the two lesions will vary genetically. Such a prospect should be taken into consideration in clinical practice, particularly when therapeutic strategies are designed.

Results presented in this study demonstrate that Cdc6 binding to the E-boxes of the *CDH1* promoter stimulates not only local heterochromatinization but also the activation of origins of replication proximal to the *CDH1* promoter. Increasing evidence, including the frequent location of replication origins near promoters, points toward an interesting interplay between replication and transcription (Sequeira-Mendes et al., 2009). The suggested aligned organization of replicons and transcription initiation sites into functional units would be teleologically more effective if the coordination of such fine procedures is regulated by a single molecular “switch.” Our data suggest that oncogenic Cdc6 undertakes this role at the *CDH1* locus and links transcriptional repression of E-cadherin to displacement of CTCF, resulting in activation of replication origins.

It has recently been proposed that CTCF is able to form unusual DNA structures through its zinc finger domains, in the form of DNA loops (MacPherson and Sadowski, 2010). Because replication origins in eukaryotes are not defined by specific sequences but rather by structural chromatin context (Antequera, 2004; Cvetic and Walter, 2005), it is likely that reorganization of these high order CTCF/chromatin structures by Cdc6 is the trigger for replicon activation, at least in the case of *CDH1* and *INK4/ARF* loci (Fig. 10). More than 13,000 CTCF binding sites are mapped (Kim et al., 2007), and  $10^4$ – $10^6$  replication origins have been suggested to occur in the genome (Cadoret et al., 2008; Sequeira-Mendes et al., 2009). In light of these observations, it would be of interest to define targets of oncogenic Cdc6 at genome-wide levels and determine whether a functional relationship between target genes, CTCF binding, and replication origins exists that associates with malignant transformation. A prediction of this prospective network is that most Cdc6-regulated targets would be either cell cycle inhibitors or genes involved in differentiation. In this mode, oncogenic Cdc6 would be expected to switch off genes that restrain cell proliferation and at the same time activate replication initiation. Whether the Cdc6 transcriptional program interferes with other transcriptional pathways remains an interesting open question. In this context, it was reported that Cdc6 interacts with c-myc, impeding E-box-dependent

transcription by changing c-myc/max heterodimer to a max/max homodimer (Takayama et al., 2000). The number of activated origins in Cdc6-transformed cells is likely to increase, in view of Cdc6's ability to trigger replication initiation when tethering to ectopic (i.e., nonorigin) sites (Takeda et al., 2005). Upon immortalization or transformation, some origins remain unchanged, and others increase their activity, whereas silent origins become activated (Di Paola et al., 2010). In line with these observations, we have found that the *CDH1* origin was dormant in immortalized but nontumorigenic P1 cells and became active upon expression of Cdc6. In contrast, we found a background activation of the *CDH1* origin of replication in A549 carcinoma cells that was further increased after expression of Cdc6. Conclusively, the oncogenic behavior of Cdc6, uncovered in this study, along with the fact that it is activated by the E2F pathway, which is commonly deregulated in cancer (Tsantoulis and Gorgoulis, 2005), renders Cdc6 a promising target for future therapeutic interventions.

## Materials and methods

### Cell lines

The A549 (human lung cancer), MCF7A (human breast cancer), T47D (human breast cancer), MDA-MB-231 (human breast cancer), MDA-MB-435 (human breast cancer), MDCK (canine kidney epithelial), and P1 (mouse skin papilloma) cell lines were maintained in DME (Invitrogen) with 10% FCS (Invitrogen), 2 mM L-glutamine (Invitrogen), and 100 µg/ml penicillin and streptomycin (Invitrogen) at 37°C and 5% CO<sub>2</sub>. HBEC3-KT (immortalized human bronchial epithelial cells) were cultured in keratinocyte serum-free medium (Invitrogen) containing 50 µg/ml bovine pituitary extract and 5 ng/ml human EGF (Invitrogen) (Sato et al., 2006 and references therein). Microphotographs were obtained after various treatments on an inverted microscope (Axiovert S100; Carl Zeiss) equipped with CP-Achromat objectives and a charge-coupled device IRIS high-resolution color video camera (SSC-C370P; Sony), whereas the Image Pro Plus v3.0 (Media Cybernetics) was used as image acquisition software.

### Plasmids and site-directed mutagenesis (Table S6)

pBabeHyg-hCdc6 was constructed by digesting pCS3-hCdc6 with BamHI and XhoI and subcloning the hCdc6-cDNA into pBabeHyg (Liontos et al., 2007). The same insert was also cloned in the BamHI and XhoI sites of pTRE2Hyg (Takara Bio Inc.). pBabeHyg-hCdc6-AAA was generated by inserting point mutations at sites A370G, G371C, C430G, and T526G as previously described (Gorgoulis et al., 1998b). These mutations led to amino acid substitutions S54A (at A370G and G371C), S74A (C430G), and S106 (T526G). pBabeHyg-hCdc6-W<sup>B</sup> was generated by point mutations at sites A1061C and A1064C. These mutations led to amino acid substitutions D284A and E285A, respectively. pCGN-hCdc6-ΔCOOH was generated by a point mutation at C1526G leading to an early termination codon. The expressed protein product is truncated at the C terminus Δ440–560 of hCdc6.

### A549-Cdc6-Tet-ON inducible system

A549 cells were transfected with the pTet-ON Advanced Vector (Takara Bio Inc.) using transfection reagent (Effectene; QIAGEN) following the manufacturer's instructions. 800 µg/ml G418 selection was initiated 4 d later, and clones emerged after 3 wk. Expression of rTA (reverse tetracycline-controlled transactivator protein) in stably transfected clones was confirmed with immunoblot analysis (antibody TetR monoclonal; Takara Bio Inc.). A549 Tet-ON clones with robust rTA expression, produced in our laboratory and donated by S. Krupenko (Medical University of South Carolina, Charleston, SC; Oleinik and Krupenko, 2003), were transfected in parallel with pTRE2Hyg-hCdc6. 300 µg/ml hygromycin selection was initiated 4 d later, and clones emerged after 3 wk. Clones with robust Cdc6 expression were selected.

### Stable transduction

A549 cells were infected with high titer retroviruses generated following transfection of 40% confluent amphotropic Phoenix cells grown in Opti-MEM (Invitrogen) with 1 µg/µl pBabeHyg and pBabeHyg-hCdc6 (Table S6)

using the calcium phosphate precipitation method. The infected cells were selected in 350 µg/ml hygromycin B for 3 wk. All experiments were performed in at least three independent replicates.

### siRNAs and transient transduction–transient transfection assays

Anti-Cdc6 and anti-CTCF siRNA (Invitrogen) transfection in P1 and A549 Cdc6 cells was performed as previously described (Liontos et al., 2009). In brief, for RNA silencing, 3 × 10<sup>5</sup> cells were plated in 60-mm dishes and, the next day, transfected using Lipofectamine 2000 (Invitrogen) with the appropriate RNAi pool (Stealth Select; Invitrogen) or the corresponding RNAi negative control (Invitrogen) according to the manufacturer's instructions. For transient transduction, 6 × 10<sup>5</sup> A549, MCF7A, MDCK, P1, or HBEC3-KT cells in 60-mm dishes were infected with retroviral pBabeHyg-hCdc6 produced in Phoenix cells and as described in the previous section (Liontos et al., 2007). The functional efficiency of the Cdc6 mutants was examined in MCF7A cells as follows: 6 × 10<sup>5</sup> cells were infected with the pBabeHyg-hCdc6-AAA and pBabeHyg-hCdc6-W<sup>B</sup>, whereas 8 × 10<sup>5</sup> cells were transiently transfected with 1 µg pCGN-hCdc6-Δ125 and pCGN-hCdc6-ΔCOOH using the Effectene transfection reagent following the manufacturer's instructions. Assay efficiency was estimated using the pCH110 plasmid containing a functional *lacZ* gene under the control of SV40 early promoter (GE Healthcare). Constructs are presented in Table S6. All experiments were performed in at least three independent replicates.

### Scratch wound assay

Cells were seeded on 60- or 100-cm<sup>2</sup> tissue-culture plastic dishes (Thermo Fisher Scientific) at 80% cell confluence, and the next day, a scratch wound was performed using a sterile 200-µl pipette tip. Phase-contrast images were taken at the starting (0 h) time point and at various time points up to 48 h using an inverted microscope (DMIRE2; Leica). Data are presented as percentages of the remaining gap distance relative to the initial gap distance. Data from three independent measurements were averaged, and the corresponding SD is also reported.

### Soft agar assay

60-mm dishes were layered with 3 ml of 0.7% (wt/vol) low melting point agarose (SeaPlaque; Lonza) dissolved in serum-containing medium. 25 × 10<sup>3</sup> A549 or A549/Cdc6 cells were then mixed with 1.6 ml of 0.35% (wt/vol) warm agar (42°C) in serum-containing medium and plated on the solidified agarose layer. Agar was added weekly, and cellular foci were enumerated on day 17. Experiments were performed in at least three independent replicates.

### Invasion assay

A549-Mock and A549-Cdc6 stable clones were seeded on top of a matrix-coated transwell (BD) at 5,000 cells per 24-well plate with serum-free medium. The transwells were embedded into complete (full serum) culture medium, and cells were allowed to invade for 24 h. At the end of the assay, the cells at the top side of the well were scraped, and cells (invading) on the bottom side of the well were stained with Giemsa, photographed, and counted. Data from three independent measurements were averaged, and the corresponding SD is also reported.

### BrdU staining

Cells grown on coverslips were incubated with 10 µM BrdU labeling reagent for 60 min at 37°C after each treatment (Liontos et al., 2007). Cells with incorporated BrdU were treated and visualized by indirect immunofluorescence (IF) as described in the corresponding methodology subsection (see Indirect IF; Liontos et al., 2007). Data from three independent measurements were averaged, and the corresponding SD is also reported.

### Growth curve analysis

Growth curve analysis was performed as previously described (Liontos et al., 2007). In brief, cells were seeded on day 0 on 60-mm Petri dishes at a density of 3 × 10<sup>5</sup> cells/dish. Every 3 d, up to day 30, cells were trypsinized and counted, and 3 × 10<sup>5</sup> cells were reseeded. The ratio of cells counted versus the cells seeded was estimated at every subculture, and the total cell number was calculated by multiplying these ratios with the number of cells seeded initially. Data from at least three independent measurements were averaged, and the corresponding SD is also reported.

### FACS

Cells were harvested with trypsinization and centrifuged at 1,000 rpm for 5 min at room temperature. The pellet was resuspended in 500 µl PBS, fixed with 80% ethanol, vortexed, and stained with 50 µg/ml propidium iodide in the presence of 5 mM MgCl<sub>2</sub> and 10 µg/ml RNase A in 10 mM Tris-HCl,

pH 7.5. DNA content was assessed on a flow cytometer (FACSCalibur; BD). Data from three independent measurements were averaged, and the corresponding SD is also reported in Fig. 1 (tables).

**Subcutaneous tumor xenografts, assessment of growth, and tumor specimens** A549-Mock and A549-Cdc6 cells were harvested, washed in PBS, and administered ( $2 \times 10^6$ ;  $n = 5$ ) at two sites in the subcutaneous tissue of the left dorsal flank of 7-wk-old male SCID mice. Tumor growth was monitored and volume (V) was calculated using the formula:  $V = a \times b \times [(a + b)/2] \times \pi/6$ . P1-Mock- and P1-Cdc6-derived mouse tumors were obtained in a similar manner as previously described (Liontos et al., 2007). In brief, cells were harvested, washed in PBS, and subcutaneously injected ( $10^6$ ;  $n = 5$ ) at two sites in the abdominal region of 7-wk-old male SCID mice. Human tumors from expanded sets of laryngeal, lung, and colon along with a new set of gastric tumors were used for immunohistochemical analysis (Liontos et al., 2007).

#### Tumor specimens

Formalin-fixed paraffin-embedded sections from 20 tumors, generated after injection of P1-Cdc6 clones in SCID mice, were analyzed. One section of each tumor was hematoxylin–eosin stained, and others were immunohistochemically analyzed. Formalin-fixed paraffin-embedded sections from expanded sets of human laryngeal, lung, and colon tumors, previously analyzed for Cdc6 expression (Liontos et al., 2007), and a new set of gastric tumors were used for immunohistochemical analysis after local ethical committee approval (Table S1).

#### Immunohistochemistry

**Antibodies.** The following antibodies were used: (a) anti-Cdc6 (H-304; class: IgG rabbit polyclonal; epitope: amino acids 257–560 of Cdc6 of human origin; 1:50; Santa Cruz Biotechnology, Inc.), (b) anti-E-cadherin (36/E-cadherin; class: IgG<sub>2a</sub>, $\kappa$  mouse monoclonal; epitope: human E-cadherin C-terminal recombinant protein; 1:100; BD), (c) antipancytokeratin (80; class: IgG1 mouse monoclonal; 1:25; Abcam), and (d) antivimentin (class: IgG rabbit polyclonal; epitope: 400 amino acids to the C terminus of human vimentin; 1:1,000; Abcam).

**Method.** Immunohistochemistry was performed using a detection kit (Laboratory Vision Ultra; Laboratory Vision) according to the manufacturer's instructions. In brief, 5-mm paraffin sections were deparaffinized by incubation in xylene and rehydrated in a graded series of ethanol aqueous solutions. Antigen retrieval was performed with 7 mM citrate buffer, pH 6.0, by microwave heating the sample for 15 min. Endogenous peroxidase activity was blocked by incubating the slides in 3% hydrogen peroxide in TBS for 10 min. The primary antibodies were incubated at 4°C overnight and then detected using the visualization system (EnVision Plus; Dako). The immunoreaction was developed with DAB (Dako) for 5 min, and hematoxylin counterstaining was used. A microscope (DM LB; Leica) equipped with a digital camera (DFC320; Leica) and N Plan objectives was used for picture acquisition. Photos were taken with the Application Suite software (version 2.2; Leica) using the automatic (software) set conditions for image acquisition.

**Evaluation.** hCdc6 positivity was ascribed when cytoplasmic and/or nuclear staining was observed (Karakaidos et al., 2004). Cytoplasmic immunoreactivity for pancytokeratin and vimentin and membranous immunostaining for E-cadherin were considered as positive.

**Controls.** Sections from previously characterized tumors (Liontos et al., 2007) served as controls for Cdc6 immunoreactivity, whereas normal mouse skin was used as control tissue for E-cadherin (Fig. 1), pancytokeratin, and vimentin immunostaining (not depicted). Staining of normal epithelial tissues was considered as an internal E-cadherin–positive control in the examined human tissues (Fig. 3). Antibodies of the corresponding IgG fraction, but of unrelated specificity, were used as negative controls.

#### Indirect IF

**Antibodies.** The antibodies used were (a) anti-E-cadherin (36/E-cadherin; class: IgG<sub>2a</sub>, $\kappa$  mouse monoclonal; epitope: human E-cadherin C-terminal recombinant protein; 1:100), (b) anti- $\beta$ -catenin (E-5; class: IgG<sub>1</sub> mouse monoclonal; epitope: amino acids 680–781 mapping at the C terminus of  $\beta$ -catenin of human origin; 1:100; Santa Cruz Biotechnology, Inc.), (c) anti-Cdc6 (180.2; class: IgG<sub>1</sub> mouse monoclonal; 1:100), and (d) anti-BrdU (mouse monoclonal; Abcam).

**Method.** Indirect IF analysis was performed according to a published protocol (Liontos et al., 2007). In brief, IF analysis was applied to cells cultured on coverslips and fixed with ice-cold methanol for 5 min. The cells were then incubated with primary antibodies at 4°C overnight. Subsequently, the antigen–primary antibody complexes were detected with an

Oregon green–conjugated goat anti-mouse or Texas red–conjugated goat anti-rabbit secondary antibody at a dilution of 1:1,000 (Invitrogen). Counterstaining was performed with 100 ng/ml DAPI (Sigma-Aldrich). A fluorescence microscope (Axiolab; Carl Zeiss) equipped with a camera (AxioCam MRm; Carl Zeiss) and Achromplan objectives was used for microscopic observation, and image acquisition was performed with AxioVision software (release 4.7.1; Carl Zeiss).

**Evaluation.** Membranous immunopositivity for E-cadherin was evaluated. For  $\beta$ -catenin, the following staining patterns were discerned: (a) membranous, as a linear staining at the cell membranes, and (b) cytoplasmic–nuclear and/or nuclear (Kotsinas et al., 2002). Cdc6-positive immunoreactivity was estimated when cytoplasmic and/or nuclear staining was observed (Karakaidos et al., 2004).

**Controls.** Normal mouse skin tissue and P1 parental cells were used as controls for E-cadherin and  $\beta$ -catenin immunostaining. Sections from previously characterized tumors served as controls for Cdc6 immunoreactivity (Liontos et al., 2007). Antibodies of the corresponding IgG fraction, but of unrelated specificity, were used as negative controls.

#### Transmission electron microscopy

Exponentially growing cells were fixed in growth medium containing 2% formaldehyde and 2% glutaraldehyde for 10 min at 37°C, washed in PBS, and postfixed in 2% formaldehyde and 2% glutaraldehyde in PBS for 2 h at room temperature. Cells were then rinsed in PBS, fixed in OsO<sub>4</sub>, dehydrated in a graded series of increased concentrations of ethanol solutions, gently scraped off with a rubber scraper, infiltrated, and finally embedded in pure Epon/Araldite resin for 24 h at 60°C (Trougakos and Margaritis, 1998; Trougakos et al., 2001). Counterstained thin resin sections were examined using an electron microscope (EM 300; Philips) operating at 60 kV. Images are shown as raw data after brightness and contrast adjustment.

#### Total protein extraction, cell fractionation, and Western blot analysis

**Total protein extraction.** Total protein extracts were obtained by homogenization in 50 mmol/liter Hepes, pH 7.5, 150 mmol/liter NaCl, 15 mmol/liter  $\beta$ -mercaptoethanol, 0.5 mmol/liter phenylmethyl sulfonyl fluoride, and 0.1% NP-40 (Sigma-Aldrich). The homogenate was centrifuged at 3,000 rpm (1,000 g) at 4°C for 5 min. The supernatant was collected and adjusted to 1  $\mu$ g/ml aprotinin, 1  $\mu$ g/ml leupeptin, and 1  $\mu$ g/ml pepstatin A (Merck; Liontos et al., 2007).

**Nuclear and membranous–cytoplasmic extracts.** Subcellular fractions consisting of nuclear and membranous–cytoplasmic protein extracts were obtained using nuclear and cytoplasmic extraction reagents (NE-PER; Thermo Fisher Scientific) with protease inhibitor (benzamidine aprotinin, leupeptin, and phenylmethyl sulfonyl fluoride) addition according to the manufacturer's instructions (Kotsinas et al., 2002).

**Antibodies and controls.** The following antibodies and the corresponding cell extracts (controls) were used: (a) Anti-Cdc6 (DCS-180; class: IgG<sub>1</sub> mouse monoclonal; epitope: recombinant, full-length hCdc6; 1:1,000; Millipore). HeLa cells were used as positive controls. (b) Anti-E-cadherin (36/E-cadherin; class: IgG<sub>2a</sub>, $\kappa$  mouse monoclonal; epitope: human E-cadherin C-terminal recombinant protein; 1:5,000). A549 cells were used as positive controls. (c) Anti- $\beta$ -actin (class: IgG rabbit polyclonal; epitope: N-terminal residues of human  $\beta$ -actin; 1:1,000; Millipore). (d) Anti-p53 (1C12; class: IgG<sub>1</sub> mouse monoclonal; epitope: residues surrounding Ser20 of human p53; 1:1,000; Cell Signaling Technology). Positive control was as previously described (Liontos et al., 2009). (e) Anti-p19 (class: IgG rabbit polyclonal; epitope: full-length mouse p19 ARF fused to GST; 1:500; Millipore). Positive controls were mouse embryo fibroblasts. (f) Anti-p16 (F-4; class: mouse monoclonal IgG<sub>1</sub>; epitope: amino acids 1–167 representing full-length p16 of mouse origin; 1:500; Santa Cruz Biotechnology, Inc.). HeLa cells were used as positive controls.

**Gel electrophoresis, blotting, and evaluation.** Protein extracts were separated by SDS-PAGE and electroblotted onto membranes (Millipore), and results were evaluated as previously reported (Liontos et al., 2007).

#### DNA–RNA analysis

**Isolation of DNA and RNA.** For DNA extraction, cells were lysed in 50 mM Tris-HCl, pH 8.0, 150 mM NaCl, 5 mM EDTA, and 1% SDS in the presence of 0.1 mg/ml proteinase K until completely dissolved. DNA was extracted with phenol/chloroform and RNase (Sigma-Aldrich) digestion followed by ethanol precipitation (Liontos et al., 2007). For RNA isolation, the TRIzol reagent (Invitrogen) was used following the manufacturer's instructions. Quality and quantity of isolated nucleic acids were estimated by spectrophotometry, fluorometry, and gel electrophoresis.

**cDNA preparation.** For reverse transcription, 2  $\mu$ g total RNA was reverse transcribed with oligo-dT (Invitrogen) and 200 U Moloney murine leukemia virus reverse transcription (Invitrogen) according to the manufacturer's instructions (Liontos et al., 2007).

### Real-time RT-PCR

**Assessment of E-cadherin levels.** Real-time RT-PCR was performed to examine the E-cadherin mRNA levels in A549, MCF7A, MDCK, P1, and HBEC3-K7 cells using  $\beta$ -microglobulin as a reference (Table S3; Liontos et al., 2007).

**Real-time PCR quantification of nascent-strand DNA.** Nascent-strand DNA was quantified with the real-time PCR system (LightCycler 480 Instrument II) using the SYBR Green I Master kit (LightCycler 480; Roche) according to the manufacturer's instructions. PCR reactions were performed in 20  $\mu$ l as previously described (Giacca et al., 1994; Rampakakis et al., 2008). Sequences and amplification conditions for all primer sets are listed in Table S4. Nonreplicating DNA from serum-starved A549 or P1 cells was included to create a standard curve for the quantification of the PCR products. A negative control without template DNA was also included.

### Isolation of nascent-strand DNA

The method applied has been previously described and extensively used with certain modifications (Tao et al., 2001; Sibani et al., 2005a,b; Callejo et al., 2006; Di Paola et al., 2006, 2010; Rampakakis et al., 2008). All DNA treatments were performed under DNase-free conditions including the use of DNase (and RNase)-free water, tubes, equipment, etc., excluding the contamination by DNases. Furthermore, the identification of the cryptic origin at the CDH1 locus was performed upon mapping a 10-kb region flanking the CDH1 promoter, wherein no other origins were detected.

Shearing of the DNA was optimized to produce DNA of  $\sim$ 20–30 kb (Di Paola et al., 2006) and not completely fragmented DNA. In this manner, the long parental DNA was sheared, whereas the short nascent DNA is not (or minimally). Identical results were obtained with either the aforementioned modified  $\lambda$  exonuclease method or the nascent-strand extrusion method, which did not involve DNA shearing (Tao et al., 2001). The technique was optimized to ensure an efficient  $\lambda$  exonuclease digestion. Under these conditions (Di Paola et al., 2006), any DNA that was not RNA primed (including an internal linear control—linearized pCR-XL-TOPO plasmid) was digested away. The methylene blue staining was used to stain the DNA markers to be able to excise and size select the 350- and 1,000-bp region containing the nascent strands.

### Luciferase reporter assay

MCF7A, P1, and induced A549-Cdc6 Tet-ON cells were seeded in 96-well plates at 2,000 cells per well with 100  $\mu$ l DME. Cells at a 90% confluency were transfected using 50  $\mu$ l Opti-MEM reduced-serum medium, 1  $\mu$ l Lipofectamine 2000 (Invitrogen), 0.2  $\mu$ g plasmid pGL2Basic, pGL2Basic-Ecad3/luciferase, pGL2Basic-EcadK1, or pGL2Basic-EcadK1/EpalMUT/EboxMUT/Ebox2MUT (Ji et al., 1997), and 0.2  $\mu$ g of the corresponding pCGN Cdc6 constructs or pCGN without an insert (Table S6). Cell extracts were obtained as recommended by the manufacturer (Luciferase Assay System; Promega). Luciferase activities were measured in a microplate reader (Safire2; Tecan). Transfection efficiency was estimated using the pCH110 plasmid containing a *lacZ* gene expressed under the control of the SV40 early promoter (GE Healthcare). All transfections were repeated three times.

### Recombinant hCdc6 production

**Cloning of hCdc6.** Cdc6 cDNA was amplified by PCR using *Pyrococcus furiosus* DNA polymerase (Agilent Technologies) from a human cDNA library. Amplification primers were 5'-ATATTGCTAGCATGCCTCAAACCCGATCC-3' (forward) and 5'-GATATGCTCGAGTTAAGGCAATCCAGTAGCTAAGA-3' (reverse). Forward and reverse primers were designed to incorporate NheI and XhoI sites at the 5' and 3' end of the amplification product, respectively. The product was NheI-XhoI double digested and ligated into the corresponding polylinker site of a dephosphorylated pET28b (EMD) vector. The generated pET28bh-Cdc6 construct contained hCdc6 fused in frame with an upstream vector sequence coding for a stretch of six histidines followed by a thrombin cleavage site (LVPRGS).

**Expression of His(6)-Cdc6.** Expression of His(6)-hCdc6 was performed in the *Escherichia coli* strain BL21(DE3) (EMD) and cotransformed with pET28bh-Cdc6 and pMBL19-ArgU plasmids (Dieci et al., 2005). Single colonies of double transformants were inoculated into 50 ml lysogeny broth medium supplemented with 100  $\mu$ g/ml ampicillin plus 50  $\mu$ g/ml kanamycin and grown overnight at 37°C. The overnight culture was diluted with lysogeny broth medium supplemented with antibiotics to a final volume of

360 ml, grown to OD<sub>595</sub> of 0.6, supplemented with 0.5 mM IPTG, and grown for another 3 h at 37°C. After IPTG induction, cells were harvested and stored at  $-80^{\circ}\text{C}$ .

**Purification of His(6)-Cdc6.** Purification of native His(6)-Cdc6 was performed with Co<sup>2+</sup>-substituted metal affinity resin according to slightly modified manufacturer's instructions (TALON; Takara Bio Inc.). In brief, the bacterial pellet obtained from 180 ml culture was thawed and resuspended in 8 ml equilibration/wash buffer (50 mM sodium phosphate and 300 mM NaCl). Lysozyme was added to a final concentration of 0.75 mg/ml. After incubation at room temperature for 30 min, bacterial lysates were sonicated, and cell debris was removed from the lysate by centrifugation. The supernatant was incubated with 0.8 ml Co<sup>2+</sup>-substituted metal affinity resin and pre-equilibrated in equilibration/wash buffer. The resin was sedimented and washed three times with equilibration/wash buffer and once with preelution buffer (50 mM sodium phosphate, 300 mM NaCl, and 20 mM imidazole). Bound proteins were eluted with the same buffer containing 450 mM imidazole. Fractions containing native His(6)-Cdc6 were identified by SDS-PAGE.

### EMSA

Nuclear extracts were obtained using the nuclear and cytoplasmic extraction kit (NE-PER) as per the manufacturer's instructions. Radioactive EMSAs were performed as previously described (Gorgoulis et al., 1998b). In brief, 1 ng  $\alpha$ -<sup>32</sup>P]ATP end-labeled oligonucleotides (Fig. S4) and 4  $\mu$ l P1 or A549 whole-cell extracts were incubated for 10 min to activate specific DNA binding of Cdc6 protein. Competition experiments were performed by preincubating activated extracts with a 50-fold molar excess of the corresponding unlabeled oligonucleotides (Fig. S4). For supershift experiments, preincubations were performed with 100 ng anti-Cdc6 antibody (C42F7; class: IgG rabbit monoclonal; Cell Signaling Technology). Protein-DNA binding reactions were resolved on a 4% nondenaturing polyacrylamide gel followed by exposure of the dried gel to x-ray film. For comparison reasons, oligonucleotides comprising the E-box 1 (Table S5) for both human and mouse CDH1 promoter were used. Selection of E-box 1—spanning oligonucleotides was also based on the coincidence with a CTCF binding site (Binding of Cdc6 to the E-boxes displaces the chromosomal insulator CTCF and histone H2A.Z triggering CDH1 promoter heterochromatinization in Results and Fig. 7 b) as well as with the mouse E-pal element.

### ChIP assay

$3 \times 10^6$  MCF7A cells transiently transfected with the corresponding Cdc6 constructs (wild type and mutants),  $3 \times 10^6$  A549 cells transiently transfected with wild-type Cdc6, and  $3 \times 10^6$  cells from corresponding P1-Cdc6 stable cell lines were cross-linked with 1% formaldehyde for 10 min at 37°C. Cross-linking was stopped by the addition of glycine to a final concentration of 125 mM for 5 min at 37°C. Cross-linked cells were washed twice in ice-cold PBS and scraped in 1 ml PBS containing protease and phosphatase inhibitors. Cells were collected by centrifugation for 5 min at 2,000 rpm, and the pellet was resuspended in 600  $\mu$ l buffer (50 mM Tris-HCl, pH 8.0, 85 mM KCl, and 0.5% NP-40) and incubated for 10 min on ice. The lysate was centrifuged for 5 min at 5,000 rpm, and the pellet was resuspended in 600  $\mu$ l lysis buffer (50 mM HEPES-KOH, pH 7.5, 150 mM NaCl, 1 mM EDTA, pH 8.0, 1% Triton X-100, 0.1% sodium deoxycholate, and 0.1% SDS) containing protease and phosphatase inhibitors. Lysates were sonicated to shear DNA to a mean fragment size of 500–1,000 bp. The debris was pelleted by 5-min centrifugation at 13,000 rpm at 4°C, and the soluble chromatin material was precleared with salmon sperm DNA/50% protein A agarose slurry (Millipore). The antibodies used for the immunoprecipitation were (a) anti-H3K9me3 (class: rabbit polyclonal IgG; Millipore), (b) antiacetyl-histone H3 (Lys9; class: rabbit polyclonal IgG; Millipore), (c) antiacetyl-histone H4 (class: rabbit polyclonal IgG; Millipore), (d) antimyc tag (9B11; class: mouse monoclonal IgG<sub>2A</sub>; Cell Signaling Technology), (e) anti-HA tag (CHIP Grade; class: rabbit polyclonal IgG; Abcam), (f) anti-CTCF (class: IgG rabbit polyclonal against amino acids 659–675 [CTNQPKQNQPATIIQVVD] of human CTCF [CCCTC-binding factor]; Millipore), and (g) anti-H2A.Z (CHIP Grade; Abcam; a gift from A.R. Nebreda, Institute for Research in Biomedicine Barcelona, Barcelona, Spain). After overnight incubation, the immune complexes were harvested with 60  $\mu$ l salmon sperm DNA/50% protein A agarose slurry for 2 h at 4°C. The beads were washed sequentially for 5 min each at room temperature in 1 ml lysis buffer without SDS, in 1 ml lysis buffer plus 500 mM NaCl, in 1 ml of buffer (10 mM Tris-HCl, pH 8.0, 1 mM EDTA, pH 8.0, 250 mM LiCl, 1% NP-40, and 1% sodium deoxycholate), and finally twice in TE (Tris-EDTA). Immune complexes were eluted with

200  $\mu$ l (two times of 100  $\mu$ l each) elution buffer (1% SDS, 50 mM Tris-HCl, pH 7.5, and 10 mM EDTA) and incubated for 5 min at 65°C. The pooled eluates were incubated with RNase for 1 and 4 h with proteinase K at 65°C. DNA was extracted by phenol/chloroform and precipitated with 10  $\mu$ g glycogen and ethanol overnight at -20°C. The DNA was resuspended in 10  $\mu$ l TE. DNA from the precipitated complexes was amplified by PCR. A 250-bp fragment of the mouse E-pal element in the E-cadherin promoter was amplified with the following primers: 5'-TAGGAAGCTGGGAAG-3' (forward) and 5'-TGCGGTCCGGCAGGG-3' (reverse; Peinado et al., 2007). A 93-bp fragment encompassing the human E-box elements 1 and 3 in the E-cadherin promoter was amplified with the following primers: 5'-CTCCAGCTTGGGTGAAAG-3' (forward) and 5'-GGGCTTTACTTGGCTGA-3' (reverse; Vesuna et al., 2008). In addition to these primers, in the T47D and MDA-MB-321 cell lines, a wider region of 216 bp was also amplified as a control for CTCF and H2A.Z binding (Table S3) as previously described (Witcher and Emerson, 2009). As inputs, we used products that corresponded to PCR reactions containing 1% of the total chromatin extract used in the immunoprecipitation reactions. All PCR amplifications were performed according to the following cycling conditions: 35 cycles at 94°C for 40 s, 58 or 65°C for 40 s, and 72°C for 40 s with DNA polymerase (GoTaq Flexi; Promega). To investigate the modification status of histones at the E-cadherin promoter, additional ChIP assays were performed in cells with or without 300 nM TSA treatment for 24 h.

#### Comet assay

Comet assay was performed as previously described (Georgakilas et al., 2010). In brief, 10<sup>5</sup> A549-Mock and A549-Cdc6 cells were seeded in 60-mm dishes. 2 d later, cells were trypsinized, centrifuged, resuspended in 2 ml PBS, and kept on ice for 10 min. Viable cells were counted using Trypan blue, and PBS was added to adjust the number of cells to 100,000 in 500  $\mu$ l PBS. 50  $\mu$ l PBS-containing cells were then mixed with equal volume of low melting agarose 1.7% (wt/vol) and were embedded in plugs. Plugs were subsequently incubated in 50 ml lysis solution (100 mM Tris-HCl, 100 mM EDTA, and 2.5 M NaCl, pH 10, with the addition of 1% [vol/vol] Triton X-100 and 10% [vol/vol] DMSO, before use) for 1 h on ice and in the dark. After completion of lysis, plugs were washed twice in TBE (Tris-boric acid-EDTA) for 1 h on ice in the dark. Finally, plugs were washed and subsequently incubated in ice-cold alkaline denaturation buffer (300 mM NaOH and 1 mM EDTA, pH 13) for 45 min on ice in the dark. For electrophoresis, plugs were mounted onto 1% agarose-coated slides that were placed into a 30-cm horizontal constant-field gel electrophoresis chamber in ice-cold alkaline denaturation buffer for 20 min at 0.7 V/cm and at 4°C. After electrophoresis, slides were dehydrated in ice-cold ethanol (100%) for 10 min and then allowed to dry in the dark. 24 h later, slides were rehydrated in 5 ml of deionized water for 10 min, and 40  $\mu$ l of diluted SYBR green (Invitrogen) was applied on each plug. Cells were observed under a fluorescence microscope (Axiolab) equipped with a monochrome UV camera (XC-EU50 CE; Sony). Analysis was conducted using the CometScore software (TriTek Corp.).

#### Cytogenetic analysis

Mouse and human cell cultures of high mitotic index were exposed to 0.1  $\mu$ g/ml colcemid (Invitrogen) for 1 h at 37°C and harvested according to routine cytogenetic protocols. Chromosome preparations were stained with appropriate FISH probes and counterstained with Vectashield containing DAPI (0.6  $\mu$ g/ml final concentration; Vector Laboratories). For the construction of representative karyotypes, we combined inverted DAPI banding and multicolor FISH (M-FISH). M-FISH was performed in 10–25 metaphase plates per cell line according to the MetaSystems. Telomere-specific peptide nucleic acid hybridization was performed using Cy3-labeled (CCCTAA)<sub>n</sub> peptide nucleic acid (analogue: 2'-deoxyoligonucleotide N3'-P5' phosphoramidate) probes (Dako) following the manufacturer's instructions. Molecular cytogenetic analyses were performed at 650 $\times$  magnification using the Isis software (MetaSystems) and a microscope (Axio Imager.Z1; Carl Zeiss) equipped with a set of six fluorochrome filters. For the evaluation of structural and numerical aberrations in P1-Cdc6 cells, we fully karyotyped two rounds of 50 complete M-FISH-stained metaphases from either Mock (pBabe) or stably Cdc6-overexpressing cells. For the evaluation of random chromosome instability in A549 cells, we fully karyotyped two rounds of 25 complete M-FISH-stained metaphases from either Mock (pBabe) or stably Cdc6-overexpressing cells and from the A549-Cdc6-Tet-ON or -Tet-OFF cell lines grown for 60 d in vitro. Comparative karyotypic analyses were performed for each pair of homologous chromosomes of the human karyotype, and all detectable structural aberrations per pair were scored. Numerical chromosomal instability was evaluated through intraploidy chromosome gains per chromosome pair.

#### Nutlin treatment

P1-Mock and P1-Cdc6/wild-type stable cell lines were treated for 48 h with two different concentrations of nutlin-3A (Sigma-Aldrich), 5 and 10  $\mu$ M. All controls were treated with DMSO. Cells were collected for FACS analysis.

#### Loss of heterozygosity (LOH) analysis

By exploiting a 15-bp difference in the *p53* gene between *Mus spretus* versus *Mus musculus* in P1 cells (Burns et al., 1991), we designed primers to perform LOH analysis. The size of the PCR product was 134/149 bp. In the A549 cells, we interrogated the intronic *p53 D17S179E* pentanucleotide microsatellite marker for LOH analysis as previously described (Liontos et al., 2009). PCR reactions were performed in a final volume of 30  $\mu$ l containing 1.5 mM MgCl<sub>2</sub>, PCR buffer (Invitrogen), a 0.2-mM concentration of each deoxyribonucleotide triphosphate, 1 U recombinant Taq polymerase (Invitrogen), and 0.3 mM primers. Primers and cycling conditions for LOH analysis in the mouse and human cell lines are described in Table S3.

**Conventional LOH analysis.** PCR products were electrophoretically separated on 10% polyacrylamide gels and stained with silver nitrate as previously reported (Gorgoulis et al., 1998a).

**Capillary electrophoresis.** The PCR products were subsequently analyzed by capillary chip electrophoresis on a microfluidics-based platform (2100 Bioanalyzer; Agilent Technologies) for further validation.

**Evaluation.** LOH was determined by densitometry, comparing the allelic ratio of the Mock DNA against that of the corresponding clones. A reduction of one of the alleles in the clones was considered to represent LOH. Alterations were confirmed by performing independent duplicate reactions.

#### Statistical analysis

Statistical analysis, comprising  $\chi^2$ , *t* test, analysis of variance, and Mann-Whitney tests, was performed with SPSS (version 12.0; IBM). Results were considered significant for *P* < 0.05.

#### Online supplemental material

Fig. S1 shows that Cdc6 overexpression induces genetic alterations (genomic instability) in P1 and A549 cells and representative results from mouse P1 cells. Fig. S2 shows representative results showing the Cdc6-induced genomic instability in A549 cells and p53 aberrations in the P1 and A549 cells. Fig. S3 shows production of nascent DNA from a replication origin adjacent to the *CDH1* promoter in A549- and P1-Cdc6 cells. Fig. S4 depicts production and purification of human recombinant Cdc6 as well as EMSAs with whole-cell extracts. Table S1 shows a summary of clinicopathological and demographic data of patients used in the current analysis. Table S2 shows immunohistochemical status of E-Cadherin and Cdc6 of the examined human carcinomas. Table S3 shows primers and annealing temperatures used in real-time RT-PCR, ChIP, and LOH analyses. Table S4 shows sequence, percentage of GC content, melting temperature, and amplicon size for all E-cadherin primers used in nascent DNA analysis. Table S5 shows oligonucleotides used in electrophoretic mobility shift assays. Table S6 shows the vectors used in this study. Online supplemental material is available at <http://www.jcb.org/cgi/content/full/jcb.201108121/DC1>.

This work is dedicated to the memory of Prof. George Thireos.

We would like to thank Dr. M. Serrano for kindly providing the pCGN, pCGNHA-Cdc6, pCGNHA-Cdc6-AAA, pCGNHA-Cdc6- $\Delta$ 125, and pCGNHA-Cdc6-W<sup>B</sup> constructs, Dr. E.R. Fearon for the pGL2Basic-Ecad3/Luciferase, pGL2Basic-EcadK1, and pGL2Basic-EcadK1/EpalMUT/EboxMUT/Ebox2MUT reporter vectors, Dr. A.R. Nebreda for providing the H2A.Z antibody, and Dr. S. Krupenko for providing p549 Tet-ON cells. Also, we would like to thank Drs. V. Zoumpourlis and E.J. Tan for their excellent technical support. Special thanks go to Dr. T. Liloglou for performing all manipulations on the HBEC3-KT and Dr. J. Mendez for critical suggestions on the manuscript.

Financial support was obtained from the European Commission Seventh Framework Programme projects Genomic Instability in Cancer and Pre-cancer (contract number 201630), Inflammation and Cancer Research in Europe (contract number 223151), INsPIRE (Integrating the Emerging Research Potential of the University of Athens Cancer Research Group in the European Research Area [REGPOT]; contract number 284460), TransPOT (contract number 285948; REGPOT), the Empeirikion Foundation, the Special Account for Research Grants-National Kapodistrian University of Athens (grants 70/4/9913, 70/4/4281, and 70/4/8916), the Ludwig Institute for Cancer Research, the Swedish Cancer Society (project number 4855-B03-01XAC), and the Cancer Research Society.

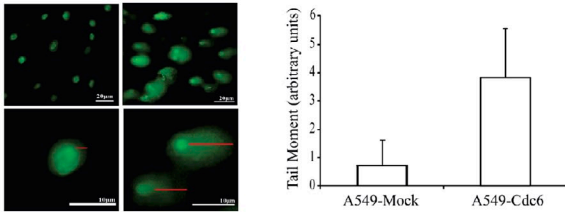
Submitted: 19 August 2011  
Accepted: 23 November 2011

## References

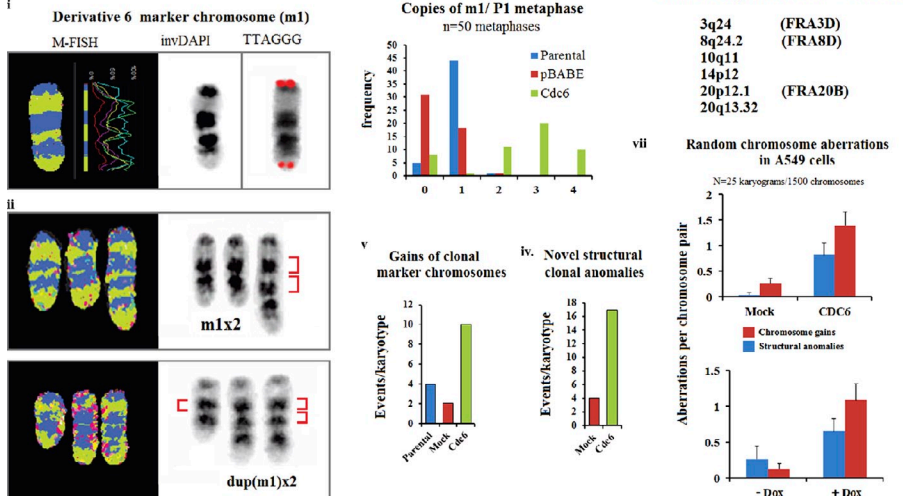
- Antequera, F. 2004. Genomic specification and epigenetic regulation of eukaryotic DNA replication origins. *EMBO J.* 23:4365–4370. <http://dx.doi.org/10.1038/sj.emboj.7600450>
- Bao, L., M. Zhou, and Y. Cui. 2008. CTCFBSDB: a CTCF-binding site database for characterization of vertebrate genomic insulators. *Nucleic Acids Res.* 36(Suppl. 1):D83–D87. <http://dx.doi.org/10.1093/nar/gkm875>
- Bartkova, J., N. Rezaei, M. Lontos, P. Karakaidos, D. Kletsas, N. Issaeva, L.V. Vassiliou, E. Kolettas, K. Niforou, V.C. Zoumpourlis, et al. 2006. Oncogene-induced senescence is part of the tumorigenesis barrier imposed by DNA damage checkpoints. *Nature.* 444:633–637. <http://dx.doi.org/10.1038/nature05268>
- Bergström, R., J. Whitehead, S. Kurukuti, and R. Ohlsson. 2007. CTCF regulates asynchronous replication of the imprinted H19/Igf2 domain. *Cell Cycle.* 6:450–454. <http://dx.doi.org/10.4161/cc.6.4.3854>
- Berx, G., and F. van Roy. 2009. Involvement of members of the cadherin superfamily in cancer. *Cold Spring Harb. Perspect. Biol.* 1:a003129. <http://dx.doi.org/10.1101/cshperspect.a003129>
- Blow, J.J., and P.J. Gillespie. 2008. Replication licensing and cancer—a fatal entanglement? *Nat. Rev. Cancer.* 8:799–806. <http://dx.doi.org/10.1038/nrc2500>
- Borlado, L.R., and J. Méndez. 2008. CDC6: from DNA replication to cell cycle checkpoints and oncogenesis. *Carcinogenesis.* 29:237–243. <http://dx.doi.org/10.1093/carcin/bgm268>
- Burns, P.A., C.J. Kemp, J.V. Gannon, D.P. Lane, R. Bremner, and A. Balmain. 1991. Loss of heterozygosity and mutational alterations of the p53 gene in skin tumours of interspecific hybrid mice. *Oncogene.* 6:2363–2369.
- Cadoret, J.C., F. Meisch, V. Hassan-Zadeh, I. Luyten, C. Guillet, L. Duret, H. Quesneville, and M.N. Prioleau. 2008. Genome-wide studies highlight indirect links between human replication origins and gene regulation. *Proc. Natl. Acad. Sci. USA.* 105:15837–15842. <http://dx.doi.org/10.1073/pnas.0805208105>
- Callejo, M., S. Sibani, D. Di Paola, G.G. Price, and M. Zannis-Hadjopoulos. 2006. Identification and functional analysis of a human homologue of the monkey replication origin ors8. *J. Cell. Biochem.* 99:1606–1615. <http://dx.doi.org/10.1002/jcb.20868>
- Cleary, J.D., S. Tomé, A. López Castel, G.B. Panigrahi, L. Foiry, K.A. Hagerman, H. Sroka, D. Chitayat, G. Gourdon, and C.E. Pearson. 2010. Tissue- and age-specific DNA replication patterns at the CTG/CAG-expanded human myotonic dystrophy type 1 locus. *Nat. Struct. Mol. Biol.* 17:1079–1087. <http://dx.doi.org/10.1038/nsmb.1876>
- Cvetic, C., and J.C. Walter. 2005. Eukaryotic origins of DNA replication: could you please be more specific? *Semin. Cell Dev. Biol.* 16:343–353. <http://dx.doi.org/10.1016/j.semcdb.2005.02.009>
- Davidson, I.F., A. Li, and J.J. Blow. 2006. Deregulated replication licensing causes DNA fragmentation consistent with head-to-tail fork collision. *Mol. Cell.* 24:433–443. <http://dx.doi.org/10.1016/j.molcel.2006.09.010>
- Dieci, G., L. Bottarelli, and S. Ottonello. 2005. A general procedure for the production of antibody reagents against eukaryotic ribosomal proteins. *Protein Pept. Lett.* 12:555–560. <http://dx.doi.org/10.2174/0929866054395860>
- Di Paola, D., G.B. Price, and M. Zannis-Hadjopoulos. 2006. Differentially active origins of DNA replication in tumor versus normal cells. *Cancer Res.* 66:5094–5103. <http://dx.doi.org/10.1158/0008-5472.CAN-05-3951>
- Di Paola, D., E. Rampakakis, M.K. Chan, D.N. Arvanitis, and M. Zannis-Hadjopoulos. 2010. Increased origin activity in transformed versus normal cells: identification of novel protein players involved in DNA replication and cellular transformation. *Nucleic Acids Res.* 38:2314–2331. <http://dx.doi.org/10.1093/nar/gkp1192>
- Falasci, A., G. Abdurashidova, O. Sandoval, S. Radulescu, G. Biamonti, and S. Riva. 2007. Molecular and structural transactions at human DNA replication origins. *Cell Cycle.* 6:1705–1712. <http://dx.doi.org/10.4161/cc.6.14.4495>
- Fu, Y., M. Sinha, C.L. Peterson, and Z. Weng. 2008. The insulator binding protein CTCF positions 20 nucleosomes around its binding sites across the human genome. *PLoS Genet.* 4:e1000138. <http://dx.doi.org/10.1371/journal.pgen.1000138>
- Georgakilas, A.G., S.M. Holt, J.M. Hair, and C.W. Loftin. 2010. Measurement of oxidatively-induced clustered DNA lesions using a novel adaptation of single cell gel electrophoresis (comet assay). *Curr. Protoc. Cell Biol.* Chapter 6:Unit 6.11.
- Giacca, M., L. Zentilin, P. Norio, S. Diviacco, D. Dimitrova, G. Contreas, G. Biamonti, G. Perini, F. Weighardt, S. Riva, et al. 1994. Fine mapping of a replication origin of human DNA. *Proc. Natl. Acad. Sci. USA.* 91:7119–7123. <http://dx.doi.org/10.1073/pnas.91.15.7119>
- Gonzalez, S., P. Klatt, S. Delgado, E. Conde, F. Lopez-Rios, M. Sanchez-Céspedes, J. Mendez, F. Antequera, and M. Serrano. 2006. Oncogenic activity of Cdc6 through repression of the INK4/ARF locus. *Nature.* 440:702–706. <http://dx.doi.org/10.1038/nature04585>
- Gorgoulis, V.G., P. Zacharatos, A. Kotsinas, T. Liloglou, A. Kyrroudi, M. Veslemes, A. Rassidakis, T.D. Halazonetis, J.K. Field, and C. Kittas. 1998a. Alterations of the p16-pRb pathway and the chromosome locus 9p21-22 in non-small-cell lung carcinomas: relationship with p53 and MDM2 protein expression. *Am. J. Pathol.* 153:1749–1765. [http://dx.doi.org/10.1016/S0002-9440\(10\)65690-8](http://dx.doi.org/10.1016/S0002-9440(10)65690-8)
- Gorgoulis, V.G., P.V. Zacharatos, E. Manolis, J.A. Ikononopoulos, A. Damalas, C. Lamprinopoulos, G.Z. Rassidakis, V. Zoumpourlis, A. Kotsinas, A.N. Rassidakis, et al. 1998b. Effects of p53 mutants derived from lung carcinomas on the p53-responsive element (p53RE) of the MDM2 gene. *Br. J. Cancer.* 77:374–384. <http://dx.doi.org/10.1038/bjc.1998.60>
- Green, B.M., K.J. Finn, and J.J. Li. 2010. Loss of DNA replication control is a potent inducer of gene amplification. *Science.* 329:943–946. <http://dx.doi.org/10.1126/science.1190966>
- Grégoire, D., K. Brodolin, and M. Méchali. 2006. HoxB domain induction silences DNA replication origins in the locus and specifies a single origin at its boundary. *EMBO Rep.* 7:812–816.
- Hajra, K.M., X. Ji, and E.R. Fearon. 1999. Extinction of E-cadherin expression in breast cancer via a dominant repression pathway acting on proximal promoter elements. *Oncogene.* 18:7274–7279. <http://dx.doi.org/10.1038/sj.onc.1203336>
- Halazonetis, T.D., V.G. Gorgoulis, and J. Bartek. 2008. An oncogene-induced DNA damage model for cancer development. *Science.* 319:1352–1355. <http://dx.doi.org/10.1126/science.1140735>
- Hanahan, D., and R.A. Weinberg. 2011. Hallmarks of cancer: the next generation. *Cell.* 144:646–674. <http://dx.doi.org/10.1016/j.cell.2011.02.013>
- Hirohashi, S. 1998. Inactivation of the E-cadherin-mediated cell adhesion system in human cancers. *Am. J. Pathol.* 153:333–339. [http://dx.doi.org/10.1016/S0002-9440\(10\)65575-7](http://dx.doi.org/10.1016/S0002-9440(10)65575-7)
- Ji, X., A.S. Woodard, D.L. Rimm, and E.R. Fearon. 1997. Transcriptional defects underlie loss of E-cadherin expression in breast cancer. *Cell Growth Differ.* 8:773–778.
- Karakaidos, P., S. Taraviras, L.V. Vassiliou, P. Zacharatos, N.G. Kastrinakis, D. Kougouli, M. Kouloukousa, H. Nishitani, A.G. Papavassiliou, Z. Lygerou, and V.G. Gorgoulis. 2004. Overexpression of the replication licensing regulators hCdt1 and hCdc6 characterizes a subset of non-small-cell lung carcinomas: synergistic effect with mutant p53 on tumor growth and chromosomal instability—evidence of E2F-1 transcriptional control over hCdt1. *Am. J. Pathol.* 165:1351–1365. [http://dx.doi.org/10.1016/S0002-9440\(10\)63393-7](http://dx.doi.org/10.1016/S0002-9440(10)63393-7)
- Kim, T.H., Z.K. Abdullaev, A.D. Smith, K.A. Ching, D.I. Loukinov, R.D. Green, M.Q. Zhang, V.V. Lobanenko, and B. Ren. 2007. Analysis of the vertebrate insulator protein CTCF-binding sites in the human genome. *Cell.* 128:1231–1245. <http://dx.doi.org/10.1016/j.cell.2006.12.048>
- Kotsinas, A., K. Evangelou, P. Zacharatos, C. Kittas, and V.G. Gorgoulis. 2002. Proliferation, but not apoptosis, is associated with distinct  $\beta$ -catenin expression patterns in non-small-cell lung carcinomas: relationship with adenomatous polyposis coli and G<sub>1</sub>-to S-phase cell-cycle regulators. *Am. J. Pathol.* 161:1619–1634. [http://dx.doi.org/10.1016/S0002-9440\(10\)64440-9](http://dx.doi.org/10.1016/S0002-9440(10)64440-9)
- Lau, E., T. Tsuji, L. Guo, S.H. Lu, and W. Jiang. 2007. The role of pre-replicative complex (pre-RC) components in oncogenesis. *FASEB J.* 21:3786–3794. <http://dx.doi.org/10.1096/fj.07-8900rev>
- Li, L.C., R.M. Chui, M. Sasaki, K. Nakajima, G. Perincher, H.C. Au, D. Nojima, P. Carroll, and R. Dahiya. 2000. A single nucleotide polymorphism in the E-cadherin gene promoter alters transcriptional activities. *Cancer Res.* 60:873–876.
- Lontos, M., M. Koutsami, M. Sideridou, K. Evangelou, D. Kletsas, B. Levy, A. Kotsinas, O. Nahum, V. Zoumpourlis, M. Kouloukousa, et al. 2007. Deregulated overexpression of hCdt1 and hCdc6 promotes malignant behavior. *Cancer Res.* 67:10899–10909. <http://dx.doi.org/10.1158/0008-5472.CAN-07-2837>
- Lontos, M., K. Niforou, G. Velimezi, K. Vougas, K. Evangelou, K. Apostolopoulou, R. Vrieli, A. Damalas, P. Kontovazenis, A. Kotsinas, et al. 2009. Modulation of the E2F1-driven cancer cell fate by the DNA damage response machinery and potential novel E2F1 targets in osteosarcomas. *Am. J. Pathol.* 175:376–391. <http://dx.doi.org/10.2353/ajpath.2009.081160>
- MacPherson, M.J., and P.D. Sadowski. 2010. The CTCF insulator protein forms an unusual DNA structure. *BMC Mol. Biol.* 11:101. <http://dx.doi.org/10.1186/1471-2199-11-101>
- Negrini, S., V.G. Gorgoulis, and T.D. Halazonetis. 2010. Genomic instability—an evolving hallmark of cancer. *Nat. Rev. Mol. Cell Biol.* 11:220–228. <http://dx.doi.org/10.1038/nrm2858>

- Norio, P., S. Kosiyatrakul, Q. Yang, Z. Guan, N.M. Brown, S. Thomas, R. Riblet, and C.L. Schildkraut. 2005. Progressive activation of DNA replication initiation in large domains of the immunoglobulin heavy chain locus during B cell development. *Mol. Cell.* 20:575–587. <http://dx.doi.org/10.1016/j.molcel.2005.10.029>
- Oleinik, N.V., and S.A. Krupenko. 2003. Ectopic expression of 10-formyltetrahydrofolate dehydrogenase in A549 cells induces G<sub>1</sub> cell cycle arrest and apoptosis. *Mol. Cancer Res.* 1:577–588.
- Peinado, H., F. Portillo, and A. Cano. 2004. Transcriptional regulation of cadherins during development and carcinogenesis. *Int. J. Dev. Biol.* 48:365–375. <http://dx.doi.org/10.1387/ijdb.041794hp>
- Peinado, H., D. Olmeda, and A. Cano. 2007. Snail, Zeb and bHLH factors in tumour progression: an alliance against the epithelial phenotype? *Nat. Rev. Cancer.* 7:415–428. <http://dx.doi.org/10.1038/nrc2131>
- Pelizon, C., F. d'Adda di Fagagna, L. Farrace, and R.A. Laskey. 2002. Human replication protein Cdc6 is selectively cleaved by caspase 3 during apoptosis. *EMBO Rep.* 3:780–784. <http://dx.doi.org/10.1093/embo-reports/kvf161>
- Pineau, P., A. Marchio, E. Cordina, P. Tiollais, and A. Dejean. 2003. Homozygous deletions scanning in tumor cell lines detects previously unsuspected loci. *Int. J. Cancer.* 106:216–223. <http://dx.doi.org/10.1002/ijc.11214>
- Rampakakis, E., D. Di Paola, and M. Zannis-Hadjopoulos. 2008. Ku is involved in cell growth, DNA replication and G1-S transition. *J. Cell Sci.* 121:590–600. <http://dx.doi.org/10.1242/jcs.021352>
- Sato, M., M.B. Vaughan, L. Girard, M. Peyton, W. Lee, D.S. Shames, R.D. Ramirez, N. Sunaga, A.F. Gazdar, J.W. Shay, and J.D. Minna. 2006. Multiple oncogenic changes (K-RAS<sup>V12</sup>, p53 knockdown, mutant EGFRs, p16 bypass, telomerase) are not sufficient to confer a full malignant phenotype on human bronchial epithelial cells. *Cancer Res.* 66:2116–2128. <http://dx.doi.org/10.1158/0008-5472.CAN-05-2521>
- Sequeira-Mendes, J., R. Díaz-Uriarte, A. Apedaile, D. Huntley, N. Brockdorff, and M. Gómez. 2009. Transcription initiation activity sets replication origin efficiency in mammalian cells. *PLoS Genet.* 5:e1000446. <http://dx.doi.org/10.1371/journal.pgen.1000446>
- Sibani, S., G.B. Price, and M. Zannis-Hadjopoulos. 2005a. Ku80 binds to human replication origins prior to the assembly of the ORC complex. *Biochemistry.* 44:7885–7896. <http://dx.doi.org/10.1021/bi047327n>
- Sibani, S., G.B. Price, and M. Zannis-Hadjopoulos. 2005b. Decreased origin usage and initiation of DNA replication in haploinsufficient HCT116 Ku80<sup>±</sup> cells. *J. Cell Sci.* 118:3247–3261. <http://dx.doi.org/10.1242/jcs.02427>
- Takayama, M., T. Taira, S.M. Iguchi-Arigo, and H. Ariga. 2000. CDC6 interacts with c-Myc to inhibit E-box-dependent transcription by abrogating c-Myc/Max complex. *FEBS Lett.* 477:43–48. [http://dx.doi.org/10.1016/S0014-5793\(00\)01756-7](http://dx.doi.org/10.1016/S0014-5793(00)01756-7)
- Takeda, D.Y., Y. Shibata, J.D. Parvin, and A. Dutta. 2005. Recruitment of ORC or CDC6 to DNA is sufficient to create an artificial origin of replication in mammalian cells. *Genes Dev.* 19:2827–2836. <http://dx.doi.org/10.1101/gad.1369805>
- Tao, L., Z. Dong, M. Zannis-Hadjopoulos, and G.B. Price. 2001. Immortalization of human WI38 cells is associated with differential activation of the c-myc origins. *J. Cell. Biochem.* 82:522–534. <http://dx.doi.org/10.1002/jcb.1173>
- Thiery, J.P., H. Acloque, R.Y. Huang, and M.A. Nieto. 2009. Epithelial-mesenchymal transitions in development and disease. *Cell.* 139:871–890. <http://dx.doi.org/10.1016/j.cell.2009.11.007>
- Trougakos, I.P., and L.H. Margaritis. 1998. The formation of the functional chorion structure of *Drosophila virilis* involves intercalation of the “middle” and “late” major chorion proteins: a general model for chorion assembly in *Drosophilidae*. *J. Struct. Biol.* 123:97–110. <http://dx.doi.org/10.1006/jsbi.1998.4999>
- Trougakos, I.P., I.S. Papassideri, G.L. Waring, and L.H. Margaritis. 2001. Differential sorting of constitutively co-secreted proteins in the ovarian follicle cells of *Drosophila*. *Eur. J. Cell Biol.* 80:271–284. <http://dx.doi.org/10.1078/0171-9335-00163>
- Tsantoulis, P.K., and V.G. Gorgoulis. 2005. Involvement of E2F transcription factor family in cancer. *Eur. J. Cancer.* 41:2403–2414. <http://dx.doi.org/10.1016/j.ejca.2005.08.005>
- Turley, E.A., M. Veisoh, D.C. Radisky, and M.J. Bissell. 2008. Mechanisms of disease: epithelial-mesenchymal transition—does cellular plasticity fuel neoplastic progression? *Nat. Clin. Pract. Oncol.* 5:280–290. <http://dx.doi.org/10.1038/nclonc1089>
- Vaziri, C., S. Saxena, Y. Jeon, C. Lee, K. Murata, Y. Machida, N. Wagle, D.S. Hwang, and A. Dutta. 2003. A p53-dependent checkpoint pathway prevents rereplication. *Mol. Cell.* 11:997–1008. [http://dx.doi.org/10.1016/S1097-2765\(03\)00099-6](http://dx.doi.org/10.1016/S1097-2765(03)00099-6)
- Vega, S., A.V. Morales, O.H. Ocaña, F. Valdés, I. Fabregat, and M.A. Nieto. 2004. Snail blocks the cell cycle and confers resistance to cell death. *Genes Dev.* 18:1131–1143. <http://dx.doi.org/10.1101/gad.294104>
- Vesuna, F., P. van Diest, J.H. Chen, and V. Raman. 2008. Twist is a transcriptional repressor of E-cadherin gene expression in breast cancer. *Biochem. Biophys. Res. Commun.* 367:235–241. <http://dx.doi.org/10.1016/j.bbr.2007.11.151>
- Witcher, M., and B.M. Emerson. 2009. Epigenetic silencing of the p16(INK4a) tumor suppressor is associated with loss of CTCF binding and a chromatin boundary. *Mol. Cell.* 34:271–284. <http://dx.doi.org/10.1016/j.molcel.2009.04.001>
- Zachariadis, M., and V.G. Gorgoulis. 2008. CDC6 (cell division cycle 6 homolog (*S. cerevisiae*)). *Atlas Genet. Cytogenet. Oncol. Haematol.* <http://AtlasGeneticsOncology.org/Genes/CDC6ID40014ch17q21.html> (accessed December 9, 2011).

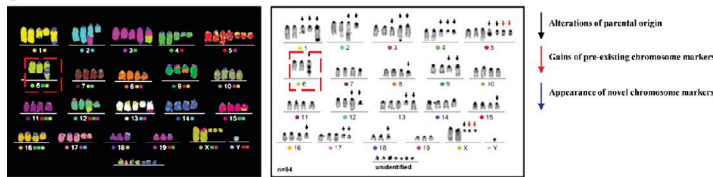
**a A549-Mock A549-Cdc6**



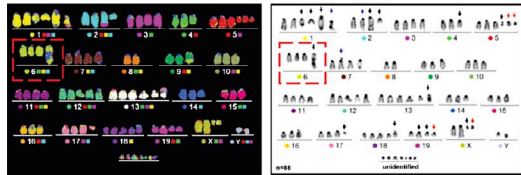
**b**



**c P1-Par**



**P1-Mock**



**P1-Cdc6**

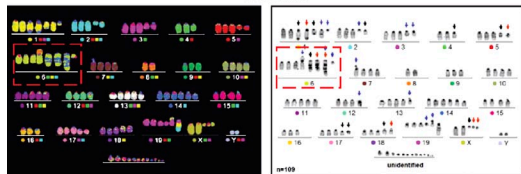
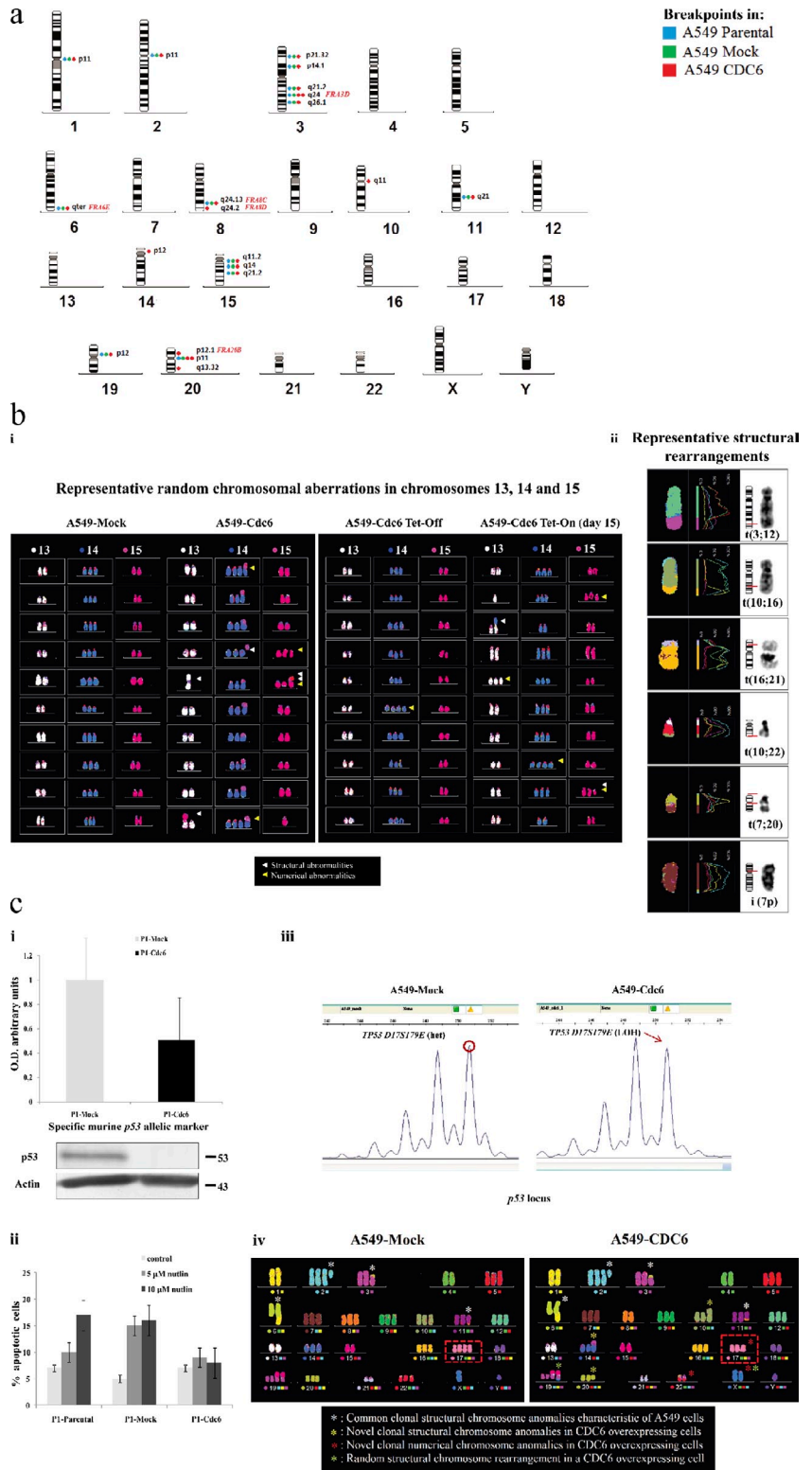


**Figure S1. Cdc6 overexpression induces genetic alterations (genomic instability) in P1 and A549 cells and representative results from mouse P1 cells.** (a) Comet assay showing DNA breaks under denaturing conditions in A549-Cdc6 cells, apparently caused via rereplication (Vaziri et al., 2003). Red lines label comet (moment) tails for length comparison reasons. (b) Summary of cytogenetic analysis in P1 (i–v) and A549 (vi–vii)-Cdc6 cells versus corresponding Mock cells. (i) Example of a mouse preexisting m1 characteristic marker (red brackets), derivative of chromosome 6 (green), rearranged with large blocks of centromeric heterochromatin of unidentified origin (blue and black) that does not display interstitial telomeric repeats (red). (ii and iii) Structural (intrachromosomal duplications) and increased numerical m1 alterations in P1-Cdc6 cells. Two rounds of 50 M-FISH–stained metaphases were evaluated. (iv and v) Acquisition of new chromosomal markers and gains in preexisting chromosomal markers are seen in P1-Cdc6 cells. Two rounds of 50 M-FISH–stained metaphases were evaluated. (vi) Novel cytogenetic breakpoints originating in A549-Cdc6 cells, with two occurring in the vicinity of common fragile sites (FRA8D and FRA20B). (vii) Increased random structural and numerical chromosomal aberrations in A549-Cdc6 and (15 d) induced A549-Cdc6–Tet-ON cells, displaying the accelerated rate of ongoing chromosomal changes (genomic instability) triggered by oncogenic Cdc6. Data obtained from molecular karyogram comparison of two rounds of 25 randomly selected mitotic nuclei of four A549 cell lines representing ~1,500 chromosomes per cell line. (c) Representative pseudocolored M-FISH/spectral karyotyping depicting structural and numerical chromosomal alterations in P1-Cdc6 cells versus parental and Mock transfected cells. Representative examples are marked by red dashed lines. invDAPI, inverted DAPI; dup, duplication; Dox, doxycycline. Error bars indicate SDs.

Downloaded from [jcb.rupress.org](http://jcb.rupress.org) on December 27, 2011

THE JOURNAL OF CELL BIOLOGY

**Figure S2. Representative results showing the Cdc6-induced genomic instability in A549 cells and p53 aberrations in the P1 and A549 cells.** (a) Collective analysis by conventional G banding and M-FISH/spectral karyotyping revealed at least five additional cytogenetically identifiable breakpoints of clonal structural chromosomal anomalies that originated after Cdc6 overexpression in A549 cells. These novel chromosomal hot spots raised the total number of genomic breakpoints from 15, originally in A549 parental and Mock cells, to 20 in Cdc6 (33.3%). Two novel clonal breakpoints in Cdc6 cells occurred in the vicinity of common aphidicolin-induced fragile sites (*FRA8D* and *FRA20B*), raising the frequency of fragile sites involved in A549 clonal structural chromosomal aberrations by 50%. (b) Representative cytogenetic analysis in A549-Cdc6 cells showing random numerical and structural chromosomal aberrations. (i and ii) 10 representative partial karyograms of the acrocentric chromosomes 13, 14, and 15 from two A549 independent experiments (15-d Cdc6 induction in A549-Tet-On cells; i) and a collection of random structural anomalies observed between Cdc6-overexpressing cells (ii) are depicted. White arrowheads depict structural anomalies; yellow arrowheads show gains of chromosomes in i, and red lines in ii show the breakpoints of random structural rearrangements (\*,  $P < 0.001$ ). (c) Cdc6-overexpressing cells demonstrate impairment of the p53 pathway. (i) p53 LOH and decreased p53 expression in P1-Cdc6 cells. (ii) Increased resistance to nutlin of P1-Cdc6 cells, a p53 activator (Shangary and Wang, 2009). (iii) p53 LOH in A549-Cdc6-grafted cells (het, heterozygous). Red circle shows signal that is subsequently reduced (red arrow). (iv) Loss of one copy of chromosome 17 as depicted by cytogenetic analysis in A549-Cdc6 cells (boxes with dashed red line). Error bars indicate SDs. Molecular markers are given in kilodaltons.



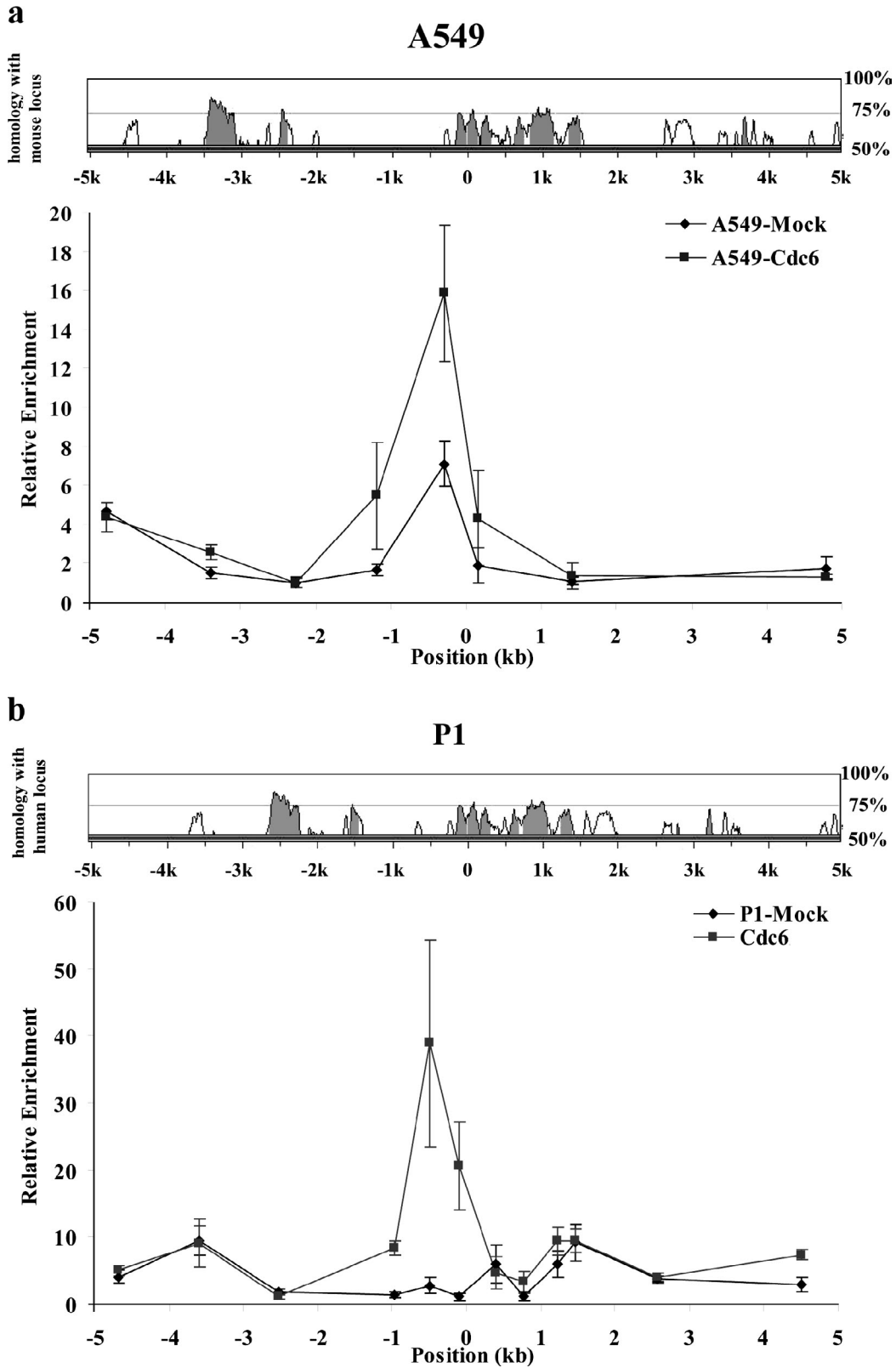


Figure S3. Production of nascent DNA from a replication origin adjacent to the *CDH1* promoter in A549- and P1-Cdc6 cells. (a and b) Values are expressed as relative enrichment of the origin-containing region compared with the origin-lacking regions and represent five experiments  $\pm$  1 SD. On top of the histograms, sequence homologies of the human and mouse *CDH1* loci are depicted using VISTA (Visualization Tool for Alignment; Frazer et al., 2004). The x axis corresponds to *CDH1* sequence length, whereas the baseline of the y axis represents a 50% degree of homology.

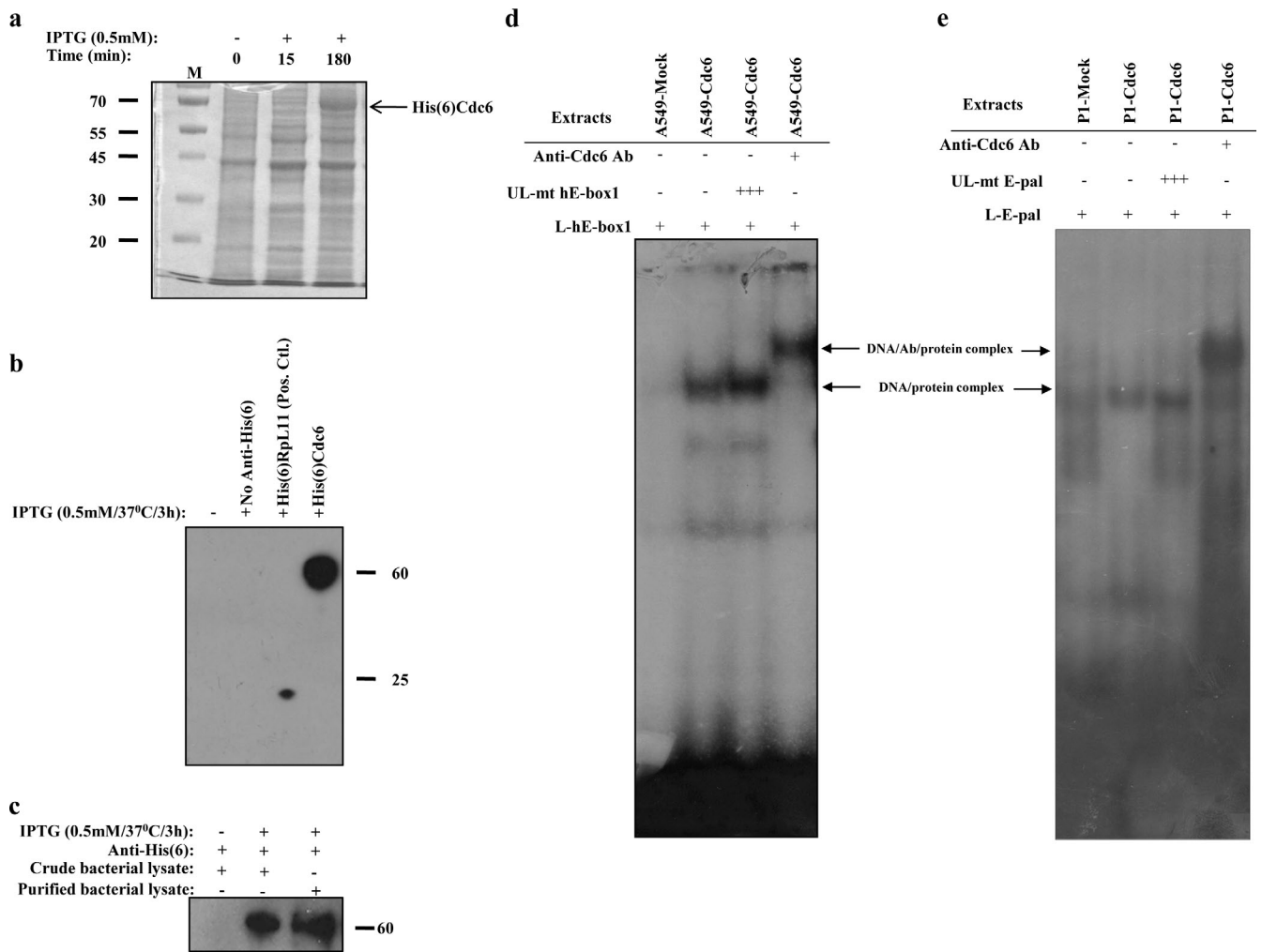


Figure S4. **Production and purification of human recombinant Cdc6 and EMSAs with whole-cell extracts.** (a) Expression of human recombinant Cdc6 in *E. coli* BL21 after IPTG induction for the indicated times. Coomassie brilliant blue staining of the gel is shown. (b) Quality control for expression of recombinant Cdc6 in bacterial lysates using anti-His immunoblotting. (Pos. Ctrl., positive control; His-tagged protein Rpl11). (c) Efficiency of purification of human recombinant Cdc6 from bacterial lysates using anti-His immunoblotting. (d and e) EMSAs depict specific binding of Cdc6 to radiolabeled human E-cadherin E-box 1 (d, left) and mouse E-pal (e, right)-negative regulatory elements in A549-Cdc6 and -P1 cells, respectively (also see Table S5). Reactions with excess unlabeled (+++) mutant oligonucleotides for the corresponding E-box 1 or E-pal elements show specificity of Cdc6 binding. A strong supershift with anti-Cdc6 antibody (Ab) demonstrates that the main bandshift is produced by Cdc6 in the cell extracts. Free probes migrate at the bottom of the gels. L, labeled oligonucleotide; UL, unlabeled oligonucleotide; mt, oligonucleotide with mutation. Molecular markers are given in kilodaltons.

Table S1. Summary of clinicopathological and demographic data of patients used in the current analysis

Patients' data	Lung (NSCLC) <sup>a</sup>	Laryngeal <sup>b</sup>	Colon <sup>c</sup>	Gastric <sup>c</sup>
Age (range in years)	45–76	48–73	39–84	42–77
Sex:				
Male	64	18	12	13
Female	11	3	8	7
Histology	Squamous, 34 Adenocarcinoma, 32 Large undifferentiated, 9	Squamous, 16 Basaloid, 3 Basosquamous, 2	Adenocarcinomas	Intestinal, 16 Mixed, 4
Total	75	21	20	20

NSCLC, nonsmall cell lung carcinoma.

<sup>a</sup>Sotiria Hospital, Athens, Greece.

<sup>b</sup>Red Cross Hospital, Athens, Greece.

<sup>c</sup>Laboratory of Histology and Embryology, University of Athens, Greece.

Table S2. Immunohistochemical status of E-Cadherin and Cdc6 of the examined human carcinomas

Cdc6	CDC6 IHC status/frequency	E-cadherin		P-value
		Membranous	Weak cytoplasmic/absent	
<b>Laryngeal carcinomas</b>				P = 0.0046
OE	13 (62%)	4 (19%)	9 (43%)	
NE	8 (38%)	8 (38%)	0 (0%)	
Total	21 (100%)	12 (57%)	9 (43%)	
<b>Nonsmall cell lung carcinomas</b>				P = 0.0001
OE	39 (52%)	11 (15%)	28 (37%)	
NE	36 (48%)	36 (48%)	0 (0%)	
Total	75 (100%)	47 (63%)	28 (37%)	
<b>Colon adenocarcinomas</b>				P = 0.0047
OE	13 (65%)	4 (20%)	9 (45%)	
NE	7 (35%)	7 (35%)	0 (0%)	
Total	20 (100%)	11 (55%)	9 (45%)	
<b>Gastric adenocarcinomas</b>				P = 0.0054
OE	14 (70%)	4 (30%)	10 (50%)	
NE	6 (30%)	6 (30%)	0 (0%)	
Total	20 (100%)	10 (50%)	10 (50%)	

Numbers in parentheses show total percentage. IHC, immunohistochemical; OE, overexpression; NE, normal expression.

Table S3. Primers and annealing temperatures used in real-time RT-PCR, ChIP, and LOH analyses

Locus	Primers (application)	Sequence	Product <i>bp</i>	Ann. Temp. °C	Reference
<i>CDH1</i> human	(quantitative real-time RT-PCR) Fw Rv	5'-TTCCCAACTCCTCCTG-3' 5'-AAACCTTGCCTCTTTGTC-3'	140	58	—
<i>CDH1</i> mouse	(quantitative real-time RT-PCR) Fw Rv	5'-CAAGGACAGCCTTCTTTTCG-3' 5'-TGGACTTCAGCGTCACTTTG-3'	165	60	—
<i>CDH1</i> canine	(quantitative real-time RT-PCR) Fw Rv	5'-AAGCGGCCTCTACAATTCA-3' 5'-AACTGGGAAATGTGAGCACC-3'	172	62	—
$\beta$ -microglobulin human	(quantitative real-time RT-PCR) Fw Rv	5'-AGCGTACTCCAAAGATTCAGTT-3' 5'-TACATGTCTCGATCCCACCTTAAC-3'	295	58	—
$\beta$ -microglobulin mouse	(quantitative real-time RT-PCR) Fw Rv	5'-GCATGGCTCGCTCGGTGAC-3' 5'-GGCGTATGTATCAGTCTCAGTG-3'	306	60	—
$\beta$ -microglobulin canine	(quantitative real-time RT-PCR) Fw Rv	5'-GCTTTGCTCCTCATCCTCC-3' 5'-CACGGCAGCTAAACTCATCC-3'	265	62	—
<i>CDH1</i> mouse	(E-pal element, ChIP) Fw Rv	5'-TAGGAAGCTGGGAAG-3' 5'-TGCGGTCGGGCAGGG-3'	250	58	Peinado et al., 2007
<i>CDH1</i> human	(E-pal element, ChIP) Fw Rv	5'-CTCCAGCTTGGGTGAAAGAG-3' 5'-GGGCTTTTACACTTGGCTGA-3'	93	65	Vesuna et al., 2008
<i>CDH1</i> human	(CTCF, ChIP) Fw Rv	5'-TAGAGGGTCACCGGTCTAT-3' 5'-TCACAGGTGCTTGCAGTTC-3'	216	52	Witcher and Emerson, 2009
<i>CDH1</i> human	(CTCF, ChIP) Fw Rv	5'-TCAGGAGCCTTAGGAGCAG-3' 5'-TCAGGCAGTCTTGTCCCTT-3'	207	52	Witcher and Emerson, 2009
<i>p53</i> mouse	(LOH) Fw Rv	5'-CCTATCCTTACCATCATCACAC-3' 5'-AGGGTAGGAACCAAAGSGCG-3'	149	52	Burns et al., 1991
<i>p53</i> human	(LOH: D17S179E) Fw Rv	5'-AGTAAGCGGAGATAGTGCCA-3' 5'-GCACTGACAAAACATCCCCT-3'	161	55	Liontos et al., 2009

Minus signs indicate no reference available. Fw, forward; Rv, reverse; Ann. Temp., annealing temperature.

Table S4. Sequence, GC content, melting temperature, and amplicon size for all E-cadherin primers used in nascent DNA analysis

Sequence name	Sequence	GC content	T <sub>m</sub>	Amplicon size
		%	°C	bp
Human #1 forward primer	5'-AAAGGGACAAGACTGCCTGAAGGA-3'	50	60.21	257
Human #1 reverse primer	5'-TCTTGCTGAGATCCAGCGCTAACA-3'	50	60.25	
Human #2 forward primer	5'-AGTGTGTGCGAAAAGTCACACAGC-3'	50	60.17	237
Human #2 reverse primer	5'-TCGTAACCTGCAGCGACTCTCAT-3'	50	59.65	
Human #3 forward primer	5'-CCATGGTGTGGCTGTGGCATTAA-3'	50	60.26	256
Human #3 reverse primer	5'-AACCTCTCTGATTCCAGGGCCTTT-3'	50	60.18	
Human #4 forward primer	5'-ACCATGCCTGGCCCTATTGTACT-3'	50	60.45	326
Human #4 reverse primer	5'-TCACTATGTTGCCGAGGCTGATCT-3'	50	59.94	
Human #5 forward primer	5'-ACTCCAGCTTGGGTGAAAGAGTGA-3'	50	60.11	174
Human #5 reverse primer	5'-TATGGGACCTGCACGGTCTGATT-3'	50	60.23	
Human #6 forward primer	5'-TGAGCTTGCAGGAAAGTCAGTTCAGA-3'	50	60.34	253
Human #6 reverse primer	5'-TTCTTGGAAAGAAGGGAAGCGGTGA-3'	50	60.33	
Human #7 forward primer	5'-ACCTGCCTGGTGTGTGACTATGT-3'	50	60.46	204
Human #7 reverse primer	5'-AAGTGGACGTCACCTCTTAGCCT-3'	50	59.35	
Human #8 forward primer	5'-ACCCAGTCCTTAGAGTTGCTGCT-3'	50	60.18	214
Human #8 reverse primer	5'-TGTGTTTCCAAGGCCAGATTGCAG-3'	50	60.15	
Mouse #1 forward primer	5'-TCAACTCACAATTGCTGGCCCTAC-3'	50	59.50	224
Mouse #1 reverse primer	5'-TTACTGGGTGAAAGAATGGGCGA-3'	50	60.44	
Mouse #2 forward primer	5'-ATTGTGTGCAACCACAGACCATCC-3'	50	59.93	190
Mouse #2 reverse primer	5'-TTAGGCTATCTGTGGCCTGGGAAA-3'	50	59.94	
Mouse #3 forward primer	5'-TAGGGAGCCTCTTGGTCTTCT-3'	50	60.05	281
Mouse #3 reverse primer	5'-TTATATCATGGCTGGGTGCAGGGA-3'	50	60.06	
Mouse #4 forward primer	5'-CAGGTTCAAATCCCAGCAACCACA-3'	50	59.95	188
Mouse #4 reverse primer	5'-AGCATCCTATGCATCCCACATCCA-3'	50	60.29	
Mouse #5 forward primer	5'-ACTAAGACAATCCAGGCCACCT-3'	50	60.14	194
Mouse #5 reverse primer	5'-TGCCACAGACCGATTGTGGAGATA-3'	50	59.92	
Mouse #6 forward primer	5'-TTGTAACCTCATGTCTCCGTGGGT-3'	50	59.89	297
Mouse #6 reverse primer	5'-AGGAGTCTAGCAGAAGTTCTGGG-3'	50	57.97	
Mouse #7 forward primer	5'-CCGCTTCCCTTCTCCAAGAAAGTTG-3'	50	59.92	288
Mouse #7 reverse primer	5'-ATCCCTTCCCTTATCTCGGATCGT-3'	50	59.04	
Mouse #8 forward primer	5'-AAGGAAAGTGGTGTCCGGAAGAGT-3'	50	60.09	295
Mouse #8 reverse primer	5'-ACCTGGGATGGAGGTAAAGTAAGC-3'	50	58.35	
Mouse #9 forward primer	5'-ATGCTGGTAGGGTGAATGGACAA-3'	50	60.38	208
Mouse #9 reverse primer	5'-GCAGGTTGGCGGTCTGAAATGAT-3'	50	60.16	
Mouse #10 forward primer	5'-TAGAGTGACTTCACAGGGTCAGCA-3'	50	59.36	154
Mouse #10 reverse primer	5'-TCCTTGGGAAAGCAGCACCTGTAT-3'	50	60.52	
Mouse #11 forward primer	5'-ACATGTTAGCCAGGCACCTAACCA-3'	50	60.48	218
Mouse #11 reverse primer	5'-TATGCAGTGGTGTGAGTGACCAGA-3'	50	59.83	
Mouse #12 forward primer	5'-TGGAACCTAACAGTGTAGCGCAGA-3'	50	60.30	189
Mouse #12 reverse primer	5'-TAGCTCTGAAAGGCCAAAGGCCAGA-3'	50	60.42	

T<sub>m</sub>, melting temperature.

Table S5. **Oligonucleotides used in electrophoretic mobility shift assays**

Species	Oligo type	Sequence
Mouse E-pal	Wild type	5'-CTGCCACCTGCAGGTGCGT-3'
	Mutant	5'-CTGCACTACTACATCTCGT-3'
Human E-box1	Wild type	5'-CTGTGGCCGGCAGGTGAAC-3'
	Mutant	5'-CTGTGGCCGG <b>ACTACT</b> AAC-3'

The underlined sequences denote the Cdc6 E-box binding region, whereas the bold denotes the same, but mutated, sequence.

Table S6. **Vectors used in this study**

Constructs	Remarks	Reference
pCGN <sup>a</sup>	Empty vector	
pCGN-HA-Cdc6 <sup>a</sup>	Parental wild-type, HA-tagged Cdc6-carrying vector	
pCGN-HA-Cdc6-AAA <sup>a</sup>	Mutation S54A/S74A/S106A, abbreviated as Cdc6-AAA, affects the three consensus Cdk phosphorylation sites 2 and 5	
pCGN-HA-Cdc6-Δ125 <sup>a</sup>	NH <sub>2</sub> -truncated Cdc6, missing amino acids 1–125	
pCGN-HA-Cdc6-W <sup>Ba</sup>	Cdc6-D284A/E285A (abbreviated W <sup>B</sup> , for Walker B mutation) affects conserved residues in the DNA-dependent ATPase domain	
pGL2Basic	Minimal promoter alone	Ji et al., 1997
pGL2Basic-Ecad3/luciferase	Carrying the –1,359 to 125 promoter region of E-cadherin	Ji et al., 1997
pGL2Pr-hRD <sup>a</sup>	Construct with minimal SV40 promoter containing the human RD <sup>INK4/ARF</sup>	
pGL2Basic-EcadK1 <sup>d</sup>	Carrying the –108 to 125 promoter region of E-cadherin	
pGL2Basic-EcadK1/EpalMUT/EboxMUT/ Ebox2MUT <sup>d</sup>	Carrying the –108 to 125 promoter region of E-cadherin with mutated E-boxes 1, 3, and 4	
pBabeHyg	Empty vector	Liontos et al., 2007
pBabeHyg-hCdc6	Parental wild-type Cdc6-carrying vector	Liontos et al., 2007
pBabeHyg-hCdc6-AAA <sup>b</sup>	A370G and G371CR mutation sites S54A Fw, 5'-AAGCCCTGCCTCTCGCCCCAGGAAACGTC-3' S54A Rv, 5'-GACGTTTCCTGGGGCGAGAGGCAGGGCTT-3' C430G mutation site S74A Fw, 5'-CTCCCCATTACCTCCTTGTGTCACCAAAGC-3' S74A Rv, 5'-GCTTTGGTGGACAACAAGGAGGTAATGGGGAG-3' T526G mutation site S106A Fw, 5'-GACAATCAGCTGACAATTAAGGCTCCTAGCAAAGAG AACTAG-3' S106A Rv, 5'-CTAGTTCTCTTTGCTAGGAGCCTTAATTGTCAGCTGATT TC-3'	
pBabeHyg-hCdc6-W <sup>Bb</sup>	A1061C and A1064C: Walker B mutation sites D284A/E285A Fw, 5'-TGATTGTGTTGGTATTGGCCGCGATGGATCAAC TGGACAG-3' D284A/ E285A Rv, 5'-CTGTCCAGTTGATCCATCGCGCCAATACCAA CACAATCA-3'	
pCGN-HA-Cdc6-ΔCOOH <sup>c</sup>	C1526G mutation site leading to a truncated C terminus Δ440–560 5'-CACATATCCCAAGTCATCTGAGAAGTTGATGGTAACAGG-3' 5'-CCTGTACCATCAACTTCTCAGATGACTGGGATATGTG-3'	
pCH110	lacZ-expressing vector under control of SV40 early promoter	

Fw, forward; Rv, reverse.

<sup>a</sup>Provided by M. Serrano (Spanish National Cancer Research Centre, Madrid, Spain; Gonzalez et al., 2006).

<sup>b</sup>Retroviral-based hCdc6-carrying vectors developed for this paper.

<sup>c</sup>pCGN-HA-Cdc6-based construct developed for this paper.

<sup>d</sup>Provided by E. Fearon (University of Michigan, Ann Arbor, MI).

## References

- Burns, P.A., C.J. Kemp, J.V. Gannon, D.P. Lane, R. Bremner, and A. Balmain. 1991. Loss of heterozygosity and mutational alterations of the p53 gene in skin tumours of interspecific hybrid mice. *Oncogene*. 6:2363–2369.
- Frazer, K.A., L. Pachter, A. Poliakov, E.M. Rubin, and I. Dubchak. 2004. VISTA: computational tools for comparative genomics. *Nucleic Acids Res.* 32(Suppl. 2):W273–W279. <http://dx.doi.org/10.1093/nar/gkh458>
- Gonzalez, S., P. Klatt, S. Delgado, E. Conde, F. Lopez-Rios, M. Sanchez-Cespedes, J. Mendez, F. Antequera, and M. Serrano. 2006. Oncogenic activity of Cdc6 through repression of the INK4/ARF locus. *Nature*. 440:702–706. <http://dx.doi.org/10.1038/nature04585>
- Ji, X., A.S. Woodard, D.L. Rimm, and E.R. Fearon. 1997. Transcriptional defects underlie loss of E-cadherin expression in breast cancer. *Cell Growth Differ.* 8:773–778.
- Liontos, M., M. Koutsami, M. Sideridou, K. Evangelou, D. Kleitsas, B. Levy, A. Kotsinas, O. Nahum, V. Zoumpourlis, M. Kouloukoussa, et al. 2007. Deregulated over-expression of hCdt1 and hCdc6 promotes malignant behavior. *Cancer Res.* 67:10899–10909. <http://dx.doi.org/10.1158/0008-5472.CAN-07-2837>
- Peinado, H., D. Olmeda, and A. Cano. 2007. Snail, Zeb and bHLH factors in tumour progression: an alliance against the epithelial phenotype? *Nat. Rev. Cancer.* 7:415–428. <http://dx.doi.org/10.1038/nrc2131>
- Shangary, S., and S. Wang. 2009. Small-molecule inhibitors of the MDM2-p53 protein-protein interaction to reactivate p53 function: a novel approach for cancer therapy. *Annu. Rev. Pharmacol. Toxicol.* 49:223–241. <http://dx.doi.org/10.1146/annurev.pharmtox.48.113006.094723>
- Vaziri, C., S. Saxena, Y. Jeon, C. Lee, K. Murata, Y. Machida, N. Wagle, D.S. Hwang, and A. Dutta. 2003. A p53-dependent checkpoint pathway prevents rereplication. *Mol. Cell.* 11:997–1008. [http://dx.doi.org/10.1016/S1097-2765\(03\)00099-6](http://dx.doi.org/10.1016/S1097-2765(03)00099-6)
- Vesuna, F., P. van Diest, J.H. Chen, and V. Raman. 2008. Twist is a transcriptional repressor of E-cadherin gene expression in breast cancer. *Biochem. Biophys. Res. Commun.* 367:235–241. <http://dx.doi.org/10.1016/j.bbrc.2007.11.151>
- Witcher, M., and B.M. Emerson. 2009. Epigenetic silencing of the p16(INK4a) tumor suppressor is associated with loss of CTCF binding and a chromatin boundary. *Mol. Cell.* 34:271–284. <http://dx.doi.org/10.1016/j.molcel.2009.04.001>